Kaon-nucleon/nuclei interaction studies at DAΦNE present and future perspectives

Kristian Piscicchia[1,2]*, Raffaele Del Grande[3,2,1]

[1] Centro Ricerche Enrico Fermi - Museo Storico della Fisica e Centro Studi e Ricerche "Enrico Fermi", 00184 Roma, Italy
[2] INFN Laboratori Nazionali di Frascati, 00044 Frascati, Italy
[3] Physik Department E62, Technische Universität München, 85748 Garching, Germany

On the behalf of the AMADEUS collaboration

***kristian.piscicchia@cref.it**

AMADEUS at LNF

INFN Istituto Nazionale di Fisica Nucleare
LABORATORI NAZIONALI DI FRASCATI

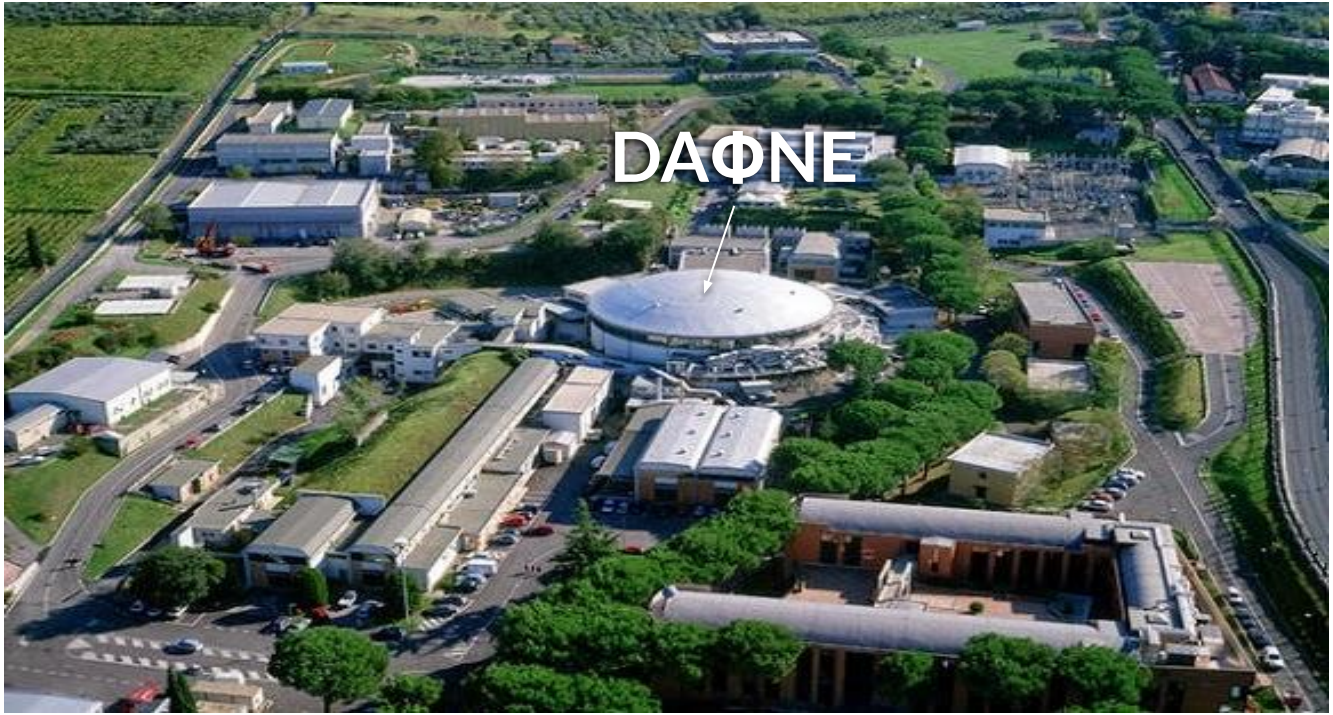

The AMADEUS collaboration

Anti-kaonic **M**atter **A**t **D**AΦNE: an **E**xperiment with **U**nravelling **S**pectroscopy

Motivation

AMADEUS (**A**ntikaonic **M**atter **A**t **D**AΦNE: an **E**xperiment with **U**nravelling **S**pectroscopy) investigates **low-energy K^- absorption in nuclei** with the aim to extract information on:

- K^-N interaction <u>above and below</u> threshold
  - Λ(1405) nature
  - kaonic bound states
  - K^-N scattering amplitudes and cross sections
- K^-NN, K^-NNN, K^-NNNN (multi-nucleon) interactions
  - essential for the determination of K^--nuclei optical potential
- In medium modification of the KbarN interaction
  - partial restoration of chiral symmetry → hadrons mass origin
  - Equation of State of Neutron Stars
  - modification of Λ(1405) and Σ(1385) properties in nuclear medium

Λ(1405) nature

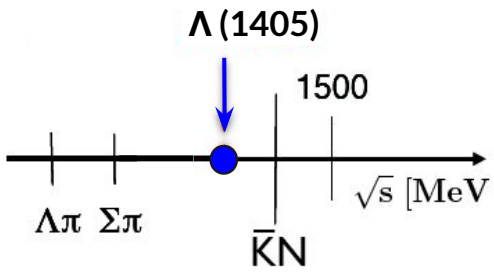

The Λ(1405) state does not fit with the simple three quarks model (*uds*) and it is commonly accepted to be **partially a K̄N bound state**.
Decay channels: $\Sigma^+\pi^-$, $\Sigma^-\pi^+$, $\Sigma^0\pi^0$

Chiral models: dynamical origin. Two poles of the scattering amplitude → pole positions is model dependent (relative contributions not measured experimentally)

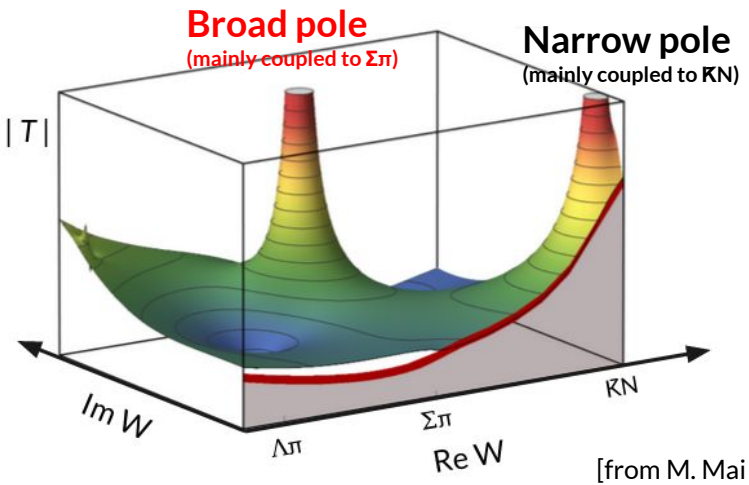

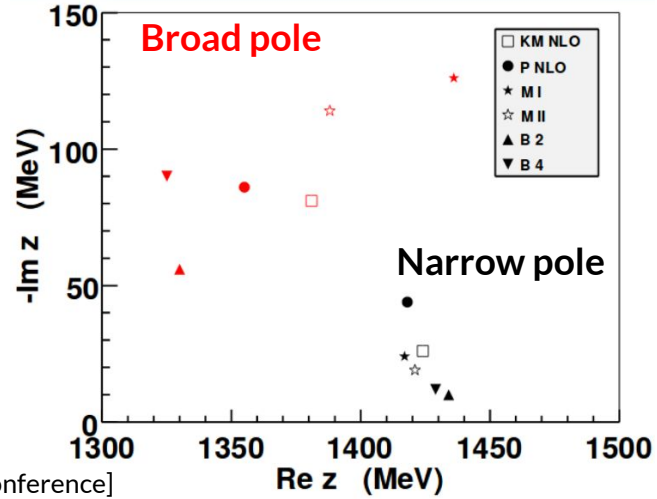

[from M. Mai talk at NSTAR19 conference]

Impact on Λ(1405) nature

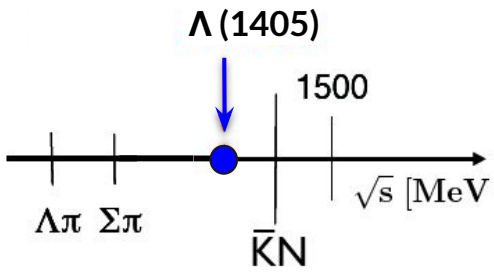

The Λ(1405) state does not fit with the simple three quarks model (*uds*) and it is commonly accepted to be **partially, a K̄N bound state**.
Decay channels: $\Sigma^+\pi^-$, $\Sigma^-\pi^+$, $\Sigma^0\pi^0$

Chiral models: dynamical origin. Two poles of the scattering amplitude → pole positions is model dependent (relative contributions not measured experimentally)

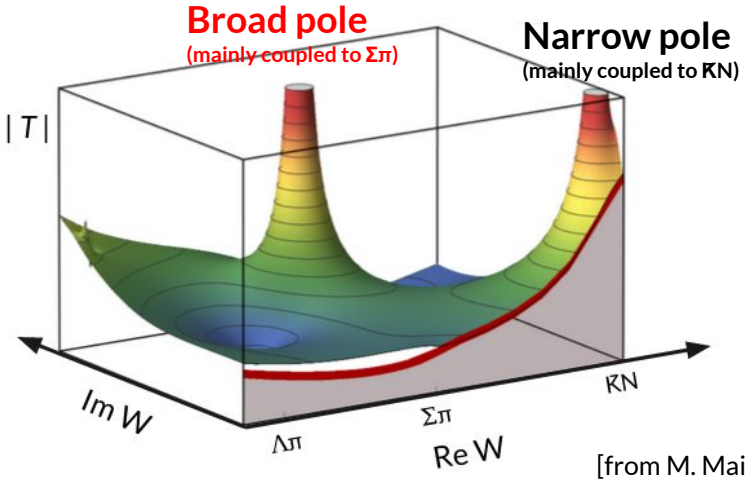

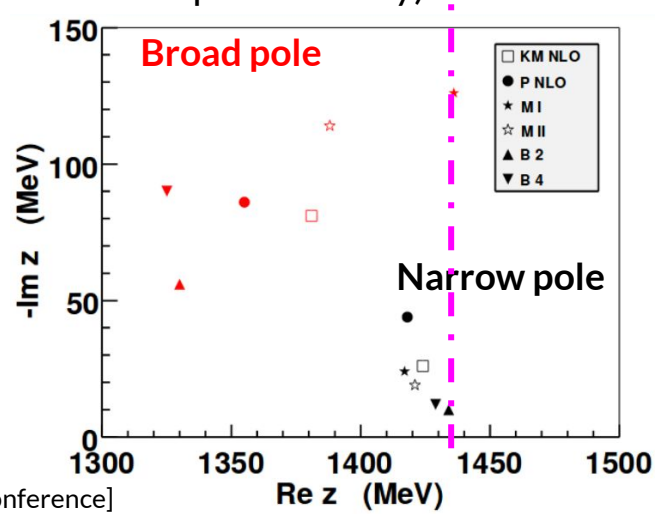

[from M. Mai talk at NSTAR19 conference]
see also Ulf-G. Meißner, *Symmetry* 12 (2020) 6, 981

Impact on Λ(1405) nature

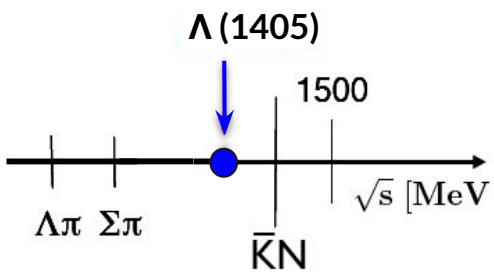

The Λ(1405) state does not fit with the simple three quarks model (*uds*) and it is commonly accepted to be **partially, a K̄N bound state**.

Single pole ansatz (Esmaili-Akaishi-Yamazaki phenomenological potential model): Very strongly attractive K̄N interaction in the I = 0 channel → existence of deeply bound kaonic states

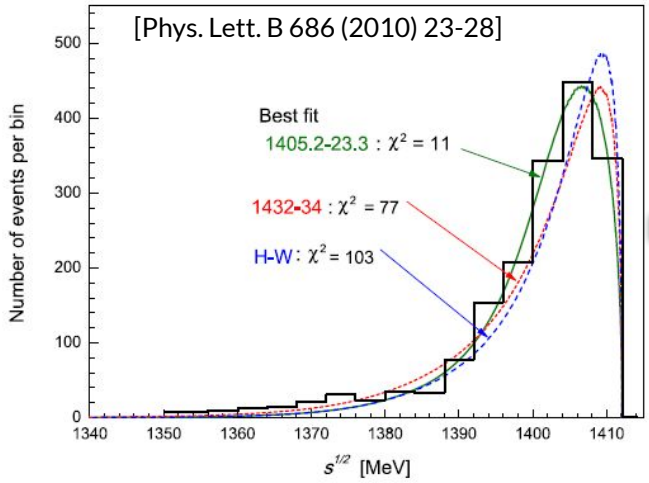

Kaonic Bound States

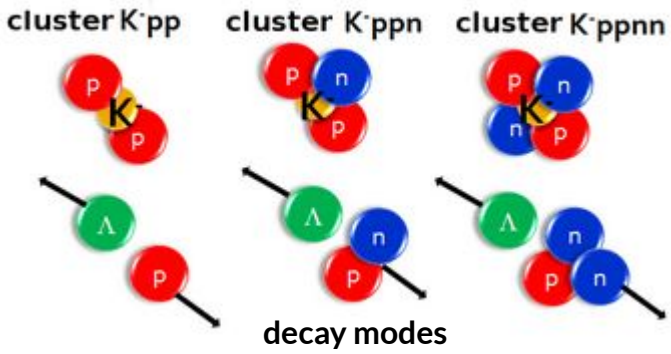

Impact on Λ(1405) nature

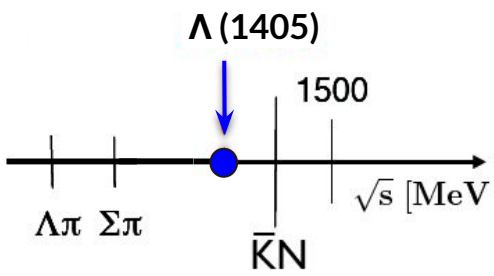

The Λ(1405) state does not fit with the simple three quarks model (*uds*) and it is commonly accepted to be **partially, a K̄N bound state**.

Single pole ansatz (Esmaili-Akaishi-Yamazaki phenomenological potential model): Very strongly attractive K̄N interaction in the I = 0 channel → existence of deeply bound kaonic states

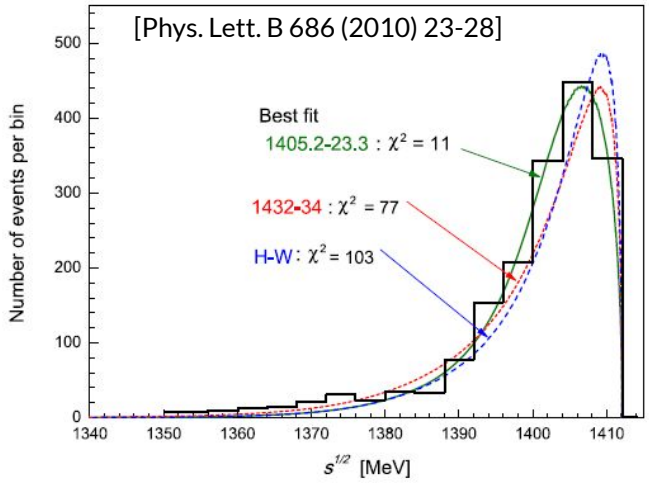

Kaonic Bound States

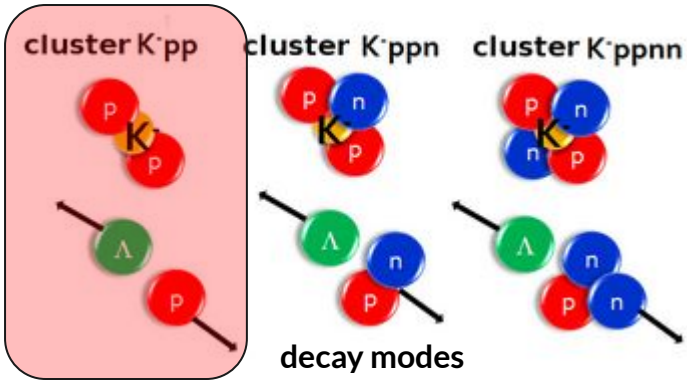

K^-pp bound state

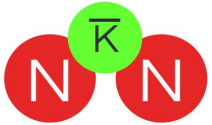

- K̄N input model is critical for the theoretical interpretation
- different bound state production mechanisms give different predictions
- **E15 gives positive evidence in K^- induced reactions in flight** (theoretical interpretation by Sekihara, Oset, Ramos)

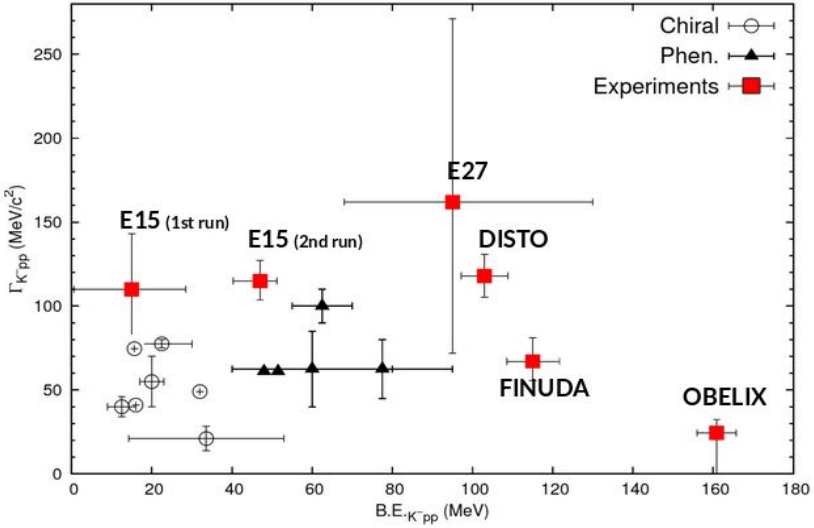

Theory

	BE (MeV)	Γ (MeV)	Reference
Dote, Hyodo, Weise	17-23	40-70	Phys.Rev.C79 (2009) 014003
Akaishi, Yamazaki	48	61	Phys.Rev.C65 (2002) 044005
Barnea, Gal, Liverts	16	41	Phys.Lett.B712 (2012) 132-137
Ikeda, Sato	60-95	45-80	Phys.Rev.C76 (2007) 035203
Ikeda, Kamano, Sato	9-16	34-46	Prog.Theor.Phys. (2010) 124(3): 533
Shevchenko, Gal, Mares	55-70	90-110	Phys.Rev.Lett.98 (2007) 082301
Revai, Shevchenko	32	49	Phys.Rev.C90 (2014) no.3, 034004
Maeda, Akaishi, Yamazaki	51.5	61	Proc.Jpn.Acad.B 89, (2013) 418
Bicudo	14.2-53	13.8-28.3	Phys.Rev.D76 (2007) 031502
Bayar, Oset	15-30	75-80	Nucl.Phys.A914 (2013) 349
Wycech, Green	40-80	40-85	Phys.Rev.C79 (2009) 014001
Sekihara, Oset, Ramos	16	72	Prog.Theor.Phys. (2016) no.12, 123D03
Sekihara, Oset, Ramos	20	80	E. Oset talk at UJ Symposium 2019

Experiments

Experiment	BE (MeV)	Γ (MeV)	Reference
FINUDA	$115\ ^{+6}_{-5}$ (stat.) $^{+3}_{-4}$ (syst.)	$67\ ^{+14}_{-11}$ (stat.) $^{+2}_{-3}$ (syst.)	PRL 94 (2005), 212303
OBELIX	160.9 ± 4.9	$< 24.4 \pm 8.0$	NPA 789 (2007), 222
E549	-	-	MPLA 23 (2008), 2520
DISTO	103 ± 3 (stat.) ± 5 (syst.)	118 ± 8 (stat.) ± 10 (syst.)	PRL 104 (2010), 132502
LEPS/SPring-8	Upper Limit		PLB 728 (2014), 616
HADES	Upper Limit		PLB 742 (2015), 242
E27	$95\ ^{+18}_{-17}$ (stat.) $^{+30}_{-21}$ (syst.)	$162\ ^{+87}_{-45}$ (stat.) $^{+66}_{-78}$ (syst.)	PTEP (2015), 021D01
AMADEUS	Upper Limit		PLB 758 (2016), 134
E15	$15\ ^{+6}_{-8}$ (stat.) ± 12 (syst.)	$110\ ^{+19}_{-17}$ (stat.) ± 27 (syst.)	PTEP (2016), 051D01
E15 (2nd run)	47 ± 3 (stat.) $^{+3}_{-6}$ (syst.)	115 ± 7 (stat.) $^{+10}_{-20}$ (syst.)	PLB 789 (2019), 620

Goals of AMADEUS

Unprecedented studies of the **low-energy charged kaons interactions in nuclear matter**: solid and gaseous targets (H, ^{4}He, ^{9}Be, ^{12}C ...) in order to obtain unique quality information about:

1. Controversial **nature of the Λ (1405)** and **K̄N amplitude below threshold**
2. **Low-energy** charged kaon **cross sections** for momenta of 100 MeV/c
3. a) Interaction of K^- with more nucleons (**multi-nucleon K^- absorptions**)

   b) possible existence of **kaonic bound states**
4. ***future*: YN scattering** → extremely **poor experimental information** from scattering data (important for the EoS of Neutron Stars)

Yπ CORRELATION STUDIES
(i.e. Λπ and Σπ and final states)

YN CORRELATION STUDIES
(i.e. Λ p, Σ^0 p, and Λ t final states)

DAΦNE the Φ factory

Istituto Nazionale di Fisica Nucleare
LABORATORI NAZIONALI DI FRASCATI

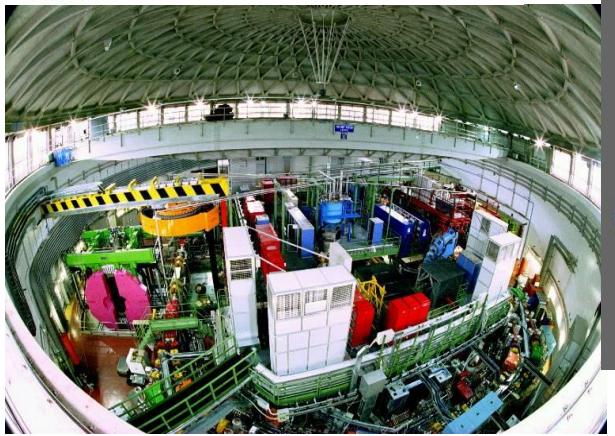

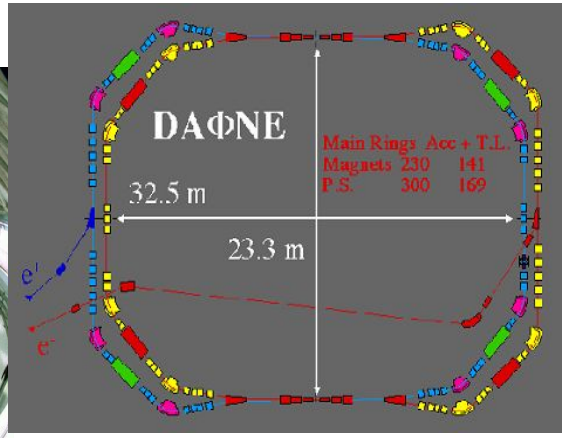

- $e^+ e^-$ at 510 MeV
- φ resonance decays at 49.2 % in K^+ K^- back to back pair
- Very low momentum (≈ 127 MeV) K^- beam
- Flux of produced kaons: about 1000/second

Best low momentum K^- factory in the world

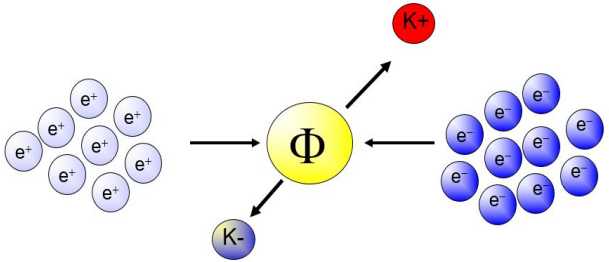

Suitable for low-energy kaon physics:
→ **Kaonic atoms** (**SIDDHARTA-2**)
→ **Kaon-nucleons/nuclei interaction** studies (**AMADEUS**)

AMADEUS step 0

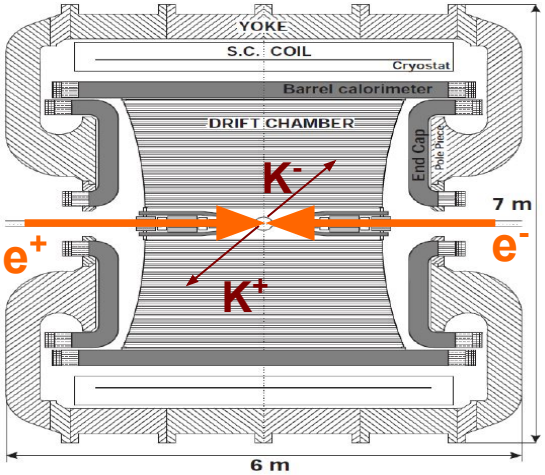

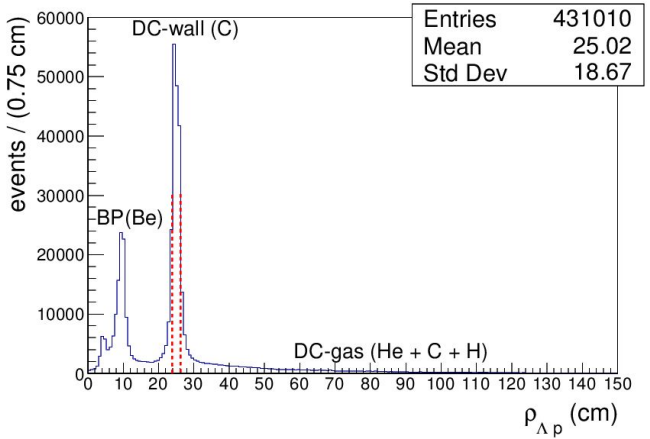

The KLOE detector

- Cylindrical drift chamber with a **4π geometry** and electromagnetic calorimeter
- **96% acceptance**
- optimized in the energy range of all **charged particles** involved
- **good performance** in detecting **photons and neutrons** checked by kloNe group

[M. Anelli et al., Nucl Inst. Meth. A 581, 368 (2007)]

Presently we use KLOE as an active target

- DC wall (750 μm C foil , 150 μm Al foil);
- DC gas (90% He, 10% C_4H_{10}).

K^- absorptions at-rest and in-flight

AT-REST

K^- absorbed from atomic orbitals

(p_K ~ 0 MeV/c)

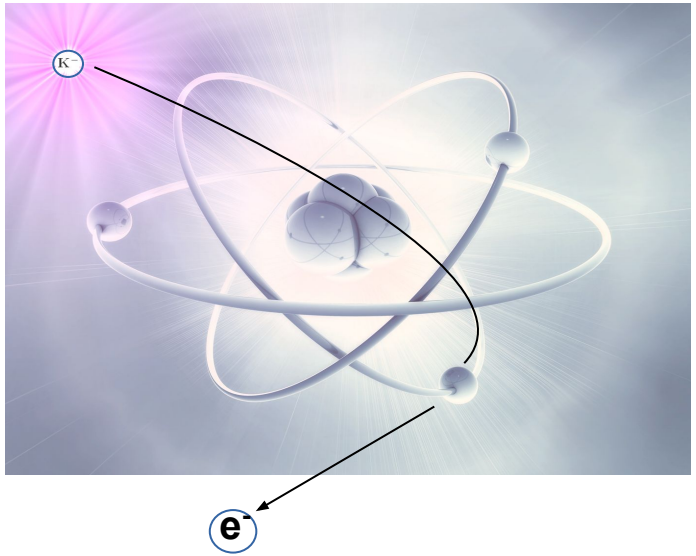

IN-FLIGHT

(p_K~ 100 MeV/c)

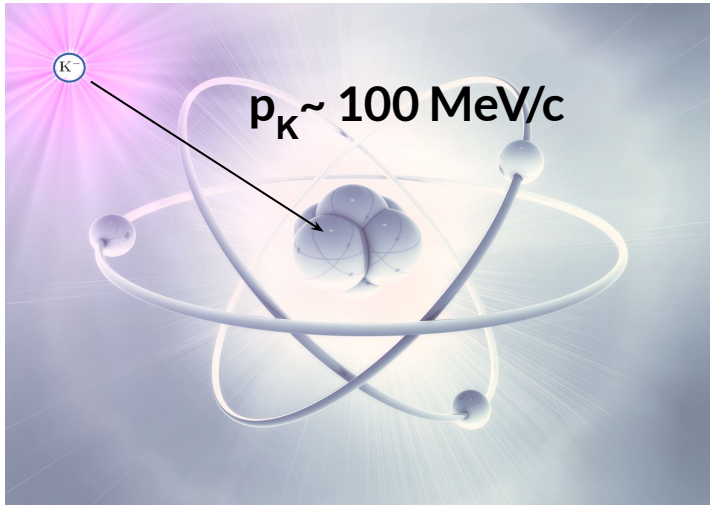

K^- multi-nucleon absorptions

In order to fit the kaonic atoms data a K^- multi-nucleon absorption term is necessary in the K^--nuclei optical potential:

$$V_{K^-}(\rho) = V_{K^-}^{(1)}(\rho) + V_{K^-}^{(2)}(\rho)$$

phen. multi-nucleon term

[E. Friedman, A. Gal, Nucl. Phys. A 959, 66 (2017)]
[Hrtánková, J. & Mareš, J. Phys. Rev. C96, 015205 (2017)]

single nucleon term from chiral models

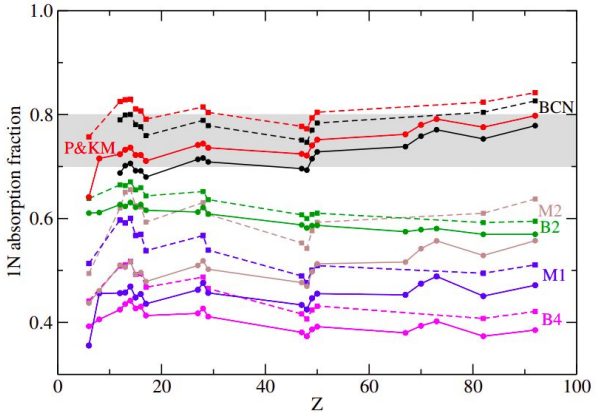

- **Single nucleon absorption (1NA):** K^- "N" $\rightarrow Y\pi$
- **Two nucleon absorption (2NA):** K^- "NN" $\rightarrow Y\,N$
- **Three nucleon absorption (3NA):** K^- "NNN" $\rightarrow Y\,(NN)$
- **Four nucleon absorption (4NA):** K^- "NNNN" $\rightarrow Y\,(NNN)$

$\rightarrow$ multi-N processes

bound nucleons = "N", "NN", "NNN", "NNNN"
bound or unbound nucleons = (NN), (NNN)
$Y = \Lambda, \Sigma$

YN correlation studies

K^- multi-nucleon absorptions are investigated by reconstructing the **hyperon-nucleon/nuclei** emitted in the final state of the process (i.e. Λp, $\Sigma^0 p$, and Λt final states)

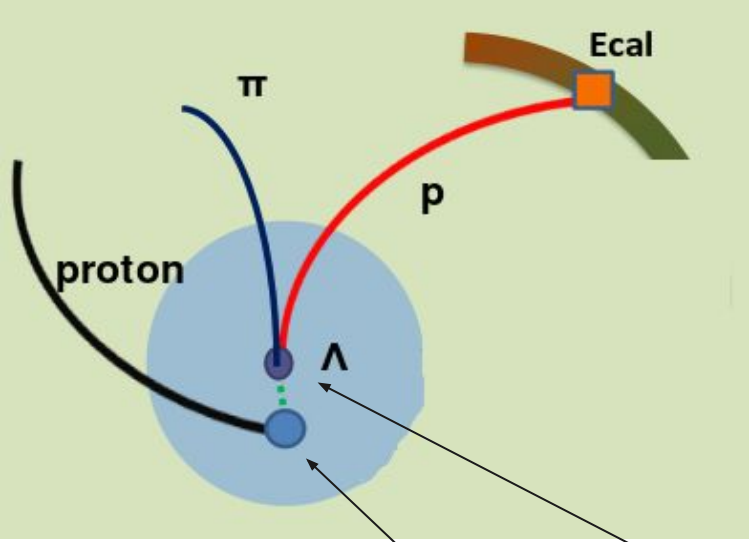

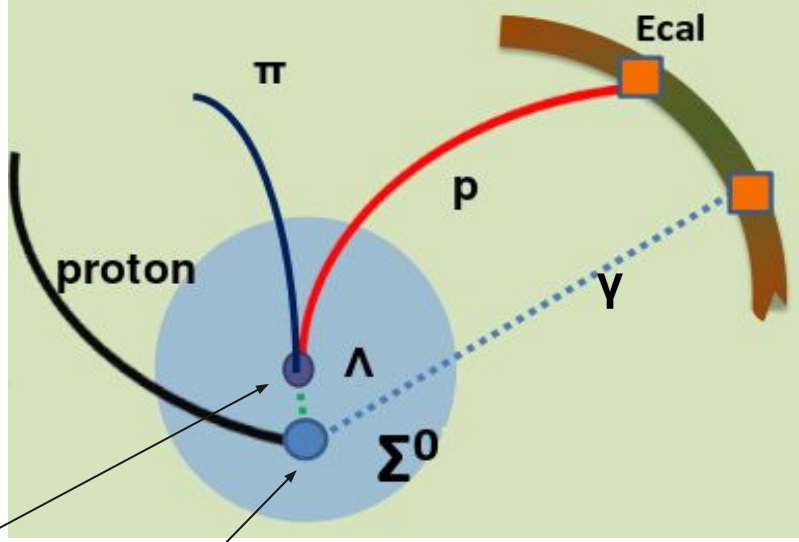

Λ decay vertex

hadronic vertex

Σ^0p analysis: $K^- + {}^{12}C \rightarrow \Sigma^0 + p + R$

Simultaneous fit of:

- Σ^0p invariant mass;
- angular correlation;
- proton momentum;
- Σ^0 momentum.

Total reduced χ^2: $\chi^2/dof = 0.85$

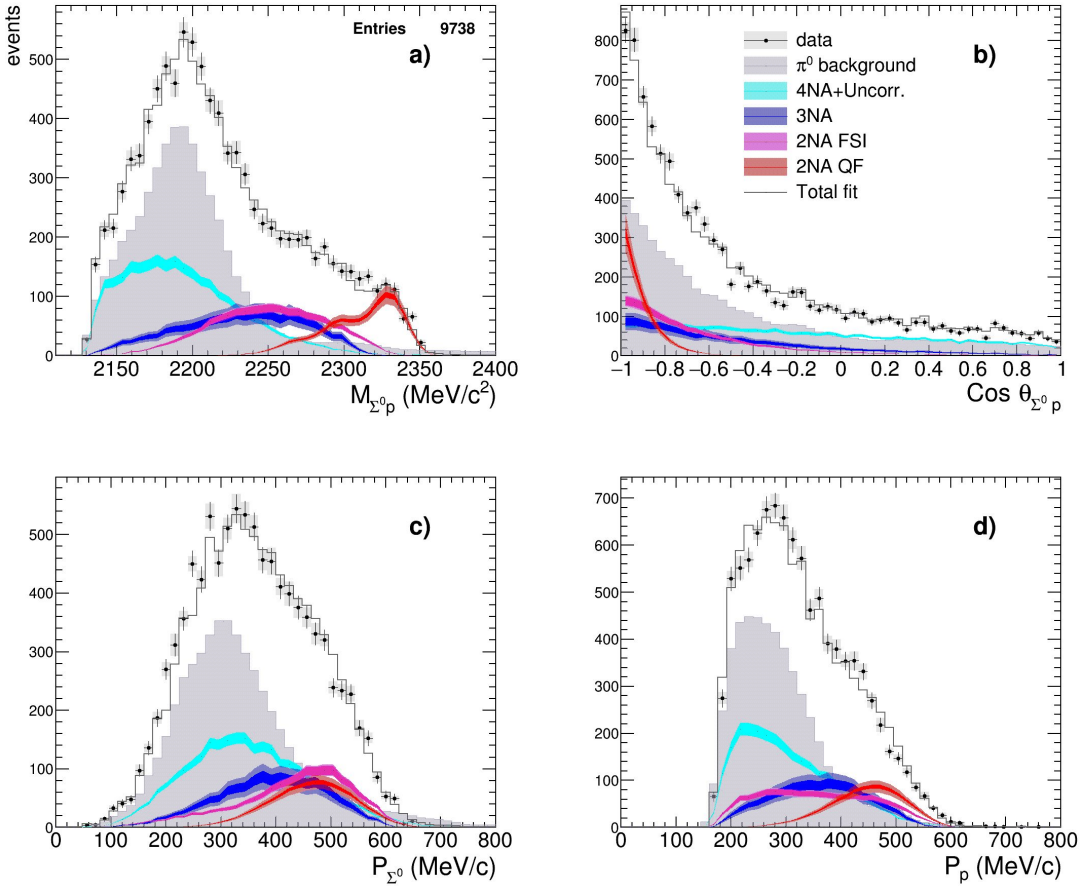

[O. Vazquez Doce, L. Fabbietti et al., Phys.Lett. B 758, 134-139 (2016)]

Σ^0p analysis: $K^- + {}^{12}C \rightarrow \Sigma^0 + p + R$

Simultaneous fit of:

- Σ^0p invariant mass;
- angular correlation;
- proton momentum;
- Σ^0 momentum.

Total reduced χ^2: $\chi^2/dof = 0.807$

Best solution:
(best χ^2 and higher yield)
- B = 45 MeV/c²
- Γ = 30 MeV/c²

Statistical significance of 1σ
(evaluated by means of F-test method)

[O. Vazquez Doce, L. Fabbietti et al., Phys.Lett. B 758, 134-139 (2016)]

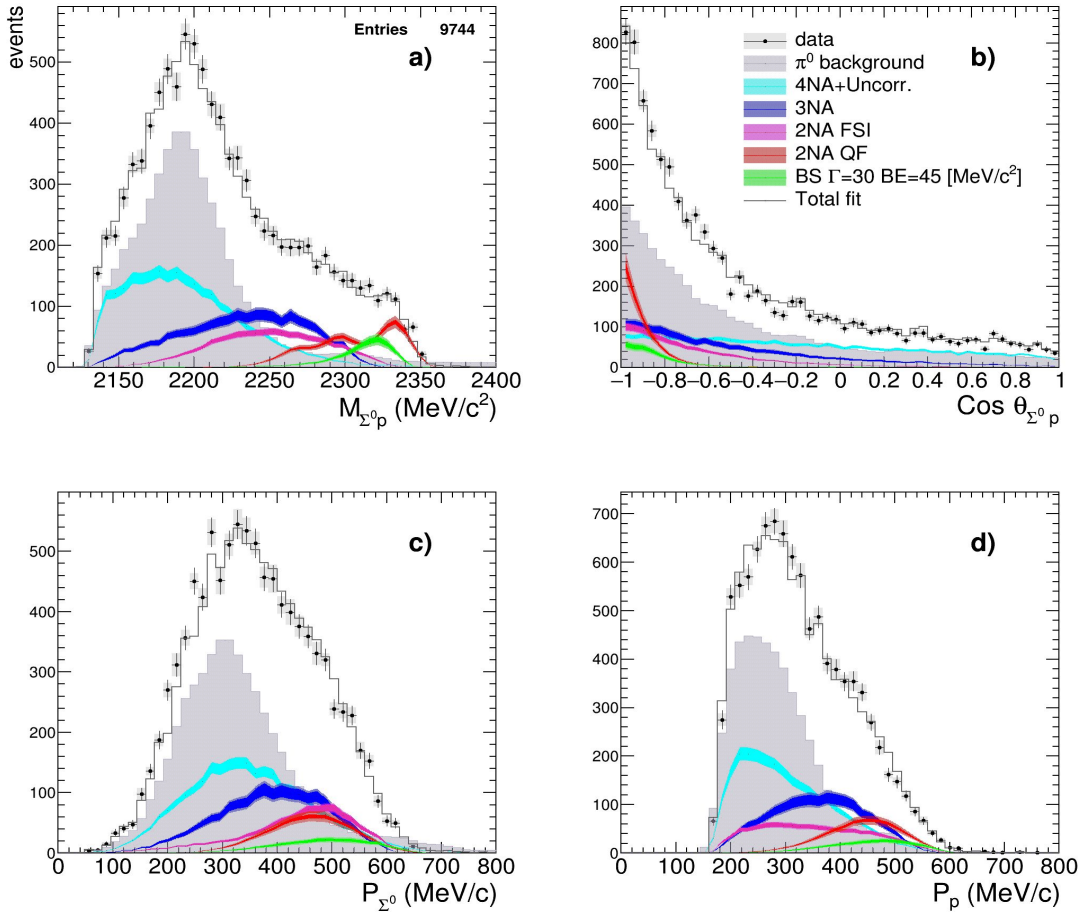

Λp analysis: $K^- + {}^{12}C \rightarrow \Lambda + p + R$

Simultaneous fit of:

- Λp invariant mass;
- angular correlation;
- proton momentum;
- Λ momentum.

Total reduced χ^2: $\chi^2/dof = 0.94$

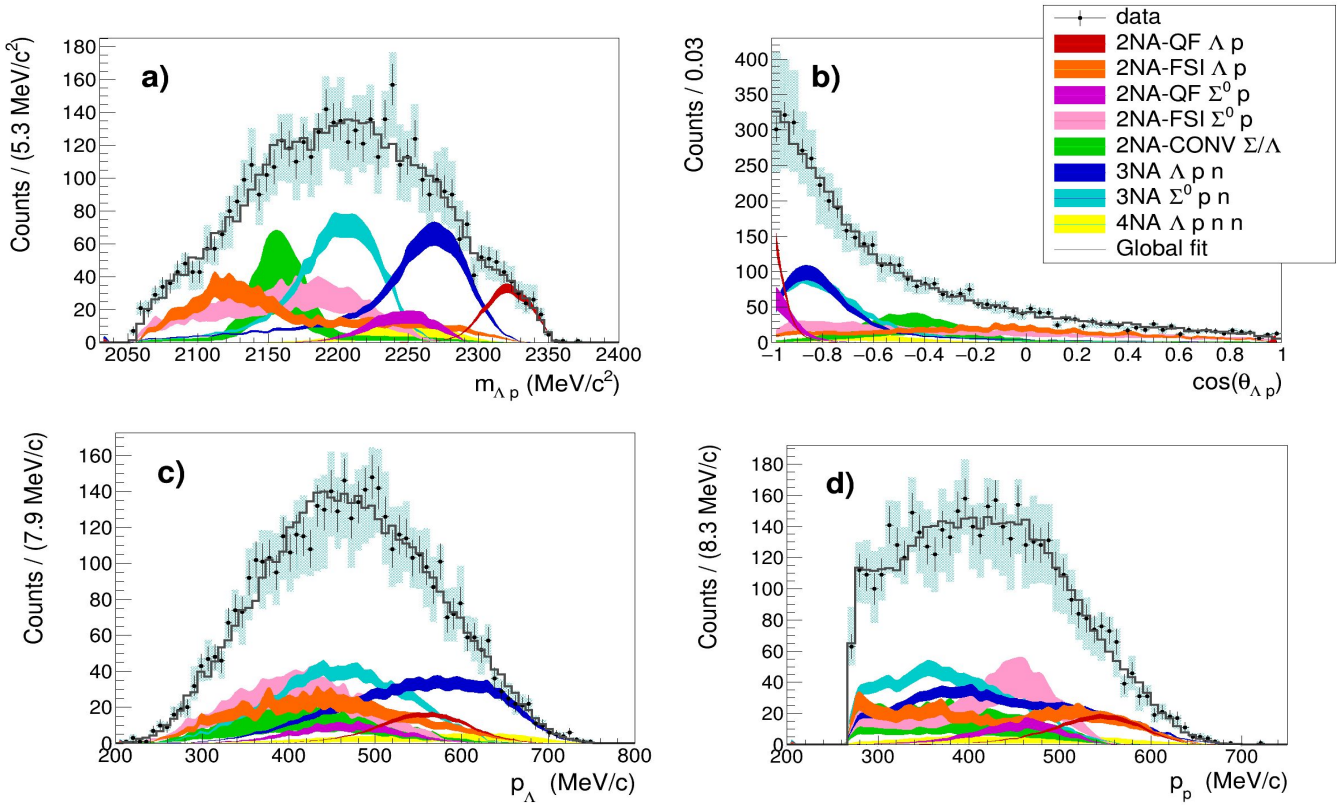

[R. Del Grande, K. Piscicchia, O. Vazquez Doce et al., Eur.Phys.J. C79 (2019) no.3, 190]
[R. Del Grande, K. Piscicchia, S. Wycech, Acta Phys. Pol. B 48 (2017) 1881]

Λp analysis: K⁻ multi-nucleon absorption BRs and σ

[R. Del Grande, K. Piscicchia, O. Vazquez Doce et al., Eur.Phys.J. C79 (2019) no.3, 190]

Process	Branching Ratio (%)	σ (mb)	@	p_K (MeV/c)
2NA-QF Λp	0.25 ± 0.02 (stat.) $^{+0.01}_{-0.02}$(syst.)	2.8 ± 0.3 (stat.) $^{+0.1}_{-0.2}$ (syst.)	@	128 ± 29
2NA-FSI Λp	6.2 ± 1.4(stat.) $^{+0.5}_{-0.6}$(syst.)	69 ± 15 (stat.) ± 6 (syst.)	@	128 ± 29
2NA-QF Σ^0p	0.35 ± 0.09(stat.) $^{+0.13}_{-0.06}$(syst.)	3.9 ± 1.0 (stat.) $^{+1.4}_{-0.7}$ (syst.)	@	128 ± 29
2NA-FSI Σ^0p	7.2 ± 2.2(stat.) $^{+4.2}_{-5.4}$(syst.)	80 ± 25 (stat.) $^{+46}_{-60}$ (syst.)	@	128 ± 29
2NA-CONV Σ/Λ	2.1 ± 1.2(stat.) $^{+0.9}_{-0.5}$(syst.)	-		
3NA Λpn	1.4 ± 0.2(stat.) $^{+0.1}_{-0.2}$(syst.)	15 ± 2 (stat.) ± 2 (syst.)	@	117 ± 23
3NA Σ^0pn	3.7 ± 0.4(stat.) $^{+0.2}_{-0.4}$(syst.)	41 ± 4 (stat.) $^{+2}_{-5}$ (syst.)	@	117 ± 23
4NA Λpnn	0.13 ± 0.09(stat.) $^{+0.08}_{-0.07}$(syst.)	-		
Global Λ(Σ^0)p	21 ± 3(stat.) $^{+5}_{-6}$(syst.)	-		

The ratio between the branching ratios of the 2NA-QF in the Λp channel and in the Σ^0p is measured to be:

$$\mathcal{R} = \frac{BR(K^- pp \to \Lambda p)}{BR(K^- pp \to \Sigma^0 p)} = 0.7 \pm 0.2(stat.)^{+0.2}_{-0.3}(syst.)$$

and the ratio between the corresponding phase spaces is $\mathcal{R}' \simeq 1.22$.

Information on the in-medium dynamics

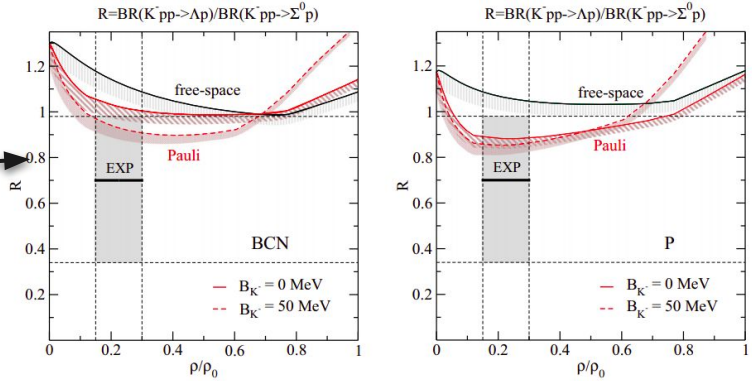

[J. Hrtánková and A. Ramos. Phys. Rev. C, 101(3):035204, 2020]

Total BR of the K^- 2NA process in ^{12}C

Hyperon-nucleon pairs produced in K^-2NA process: **Λp Λn $\Sigma^0 p$ $\Sigma^0 n$ $\Sigma^+ n$ $\Sigma^- p$ $\Sigma^- n$**

BCN calculation at 0.3 ρ_0 (baryon density in ^{12}C) → BR(K^-2NA → YN) = (15.4 ± 2.2) %
[J. Hrtánková and A. Ramos. Phys. Rev. C, 101(3):035204, 2020]

Process	Branching Ratio (%)
2NA-QF Λp	0.25 ± 0.02 (stat.) $^{+0.01}_{-0.02}$(syst.)
2NA-FSI Λp	6.2 ± 1.4(stat.) $^{+0.5}_{-0.6}$(syst.)
2NA-QF $\Sigma^0 p$	0.35 ± 0.09(stat.) $^{+0.13}_{-0.06}$(syst.)
2NA-FSI $\Sigma^0 p$	7.2 ± 2.2(stat.) $^{+4.2}_{-5.4}$(syst.)
2NA-CONV Σ/Λ	2.1 ± 1.2(stat.) $^{+0.9}_{-0.5}$(syst.)
3NA Λpn	1.4 ± 0.2(stat.) $^{+0.1}_{-0.2}$(syst.)
3NA $\Sigma^0 pn$	3.7 ± 0.4(stat.) $^{+0.2}_{-0.4}$(syst.)
4NA Λpnn	0.13 ± 0.09(stat.) $^{+0.08}_{-0.07}$(syst.)
Global $\Lambda(\Sigma^0)p$	21 ± 3(stat.) $^{+5}_{-6}$(syst.)

We measure a total K^-2NA BR in ^{12}C

→ (16.1 ± 2.9(stat.) $^{+4.3}_{-5.5}$ (syst.))%,

Λp and $\Sigma^0 p$ pairs in the final state….
….information on the remaining YN pairs provided by FSI e Conversion reactions

[R. Del Grande, K. Piscicchia et al., 2020 Phys. Scr.95 084012]

Total BR of the K^- 2NA process in ^{12}C

FSI and Conversion reactions contributing to the measured BRs

	primary interaction	secondary interaction
2NA-FSI Λp	$K^-pn \to \Lambda n$	$\Lambda p \to \Lambda p$
	$K^-pn \to \Lambda n$	$n p \to n p$
	$K^-pp \to \Lambda p$	$\Lambda N \to \Lambda N$
	$K^-pp \to \Lambda p$	$p N \to p N$
2NA-FSI Σ^0p	$K^-pn \to \Sigma^0 n$	$\Sigma^0 p \to \Sigma^0 p$
	$K^-pn \to \Sigma^0 n$	$n p \to n p$
	$K^-pp \to \Sigma^0 p$	$\Sigma^0 N \to \Sigma^0 N$
	$K^-pp \to \Sigma^0 p$	$p N \to p N$
2NA-Conv.	$K^-pn \to \Sigma^0 n$	$\Sigma^0 p \to \Lambda p$
	$K^-pp \to \Sigma^0 p$	$\Sigma^0 p \to \Lambda p$
	$K^-pp \to \Sigma^0 p$	$\Sigma^0 n \to \Lambda n$
	$K^-pn \to \Sigma^- p$	$\Sigma^- p \to \Lambda n$
	$K^-pp \to \Sigma^+ n$	$\Sigma^+ n \to \Lambda p$

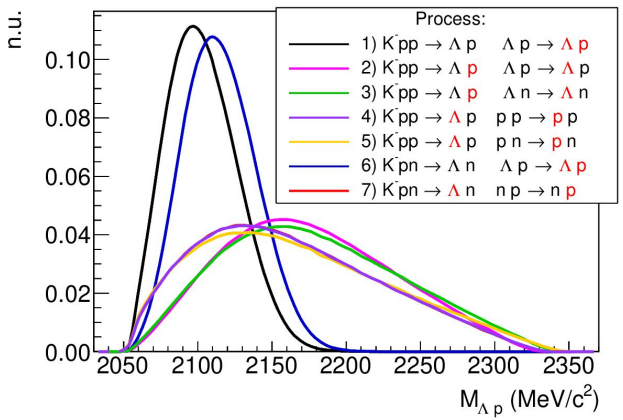

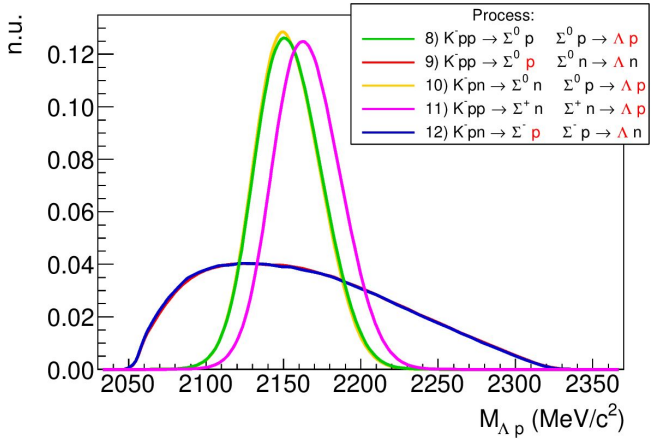

red = detected Λp pair

Total BR of the K^- 2NA process in ^{12}C

the only missing components are:

- BR($\Sigma^- n$) = (0.12 ± 0.01(syst.))%
- BR(QF-Λn + QF-$\Sigma^0 n$) = (0.76 ± 0.09(stat.) $^{+0.13}_{-0.06}$ (syst.))%
- BR(FSI-Λn + FSI-$\Sigma^0 n$) = (1.62 ± 0.04(stat.) $^{+0.22}_{-0.21}$ (syst.))%
- BR(no conv Σ^+ and Σ^-) = (3.04 ± 0.03(stat.) ± 0.92(syst.))%

→ **(5.5 ± 0.1(stat.) $^{+1.0}_{-0.9}$ (syst.))%**

[R. Del Grande, K. Piscicchia et al., 2020 Phys. Scr.95 084012]
[R. Del Grande, K. Piscicchia et al., *Few Body Syst.* 62 (2021) 1, 7]

Including the missing components the total BR of the K^-2NA is:

$$\mathrm{BR}(\mathrm{K}^-2\mathrm{NA} \to \mathrm{YN}) = (21.6 \pm 2.9(\mathrm{stat.})^{+4.4}_{-5.6}(\mathrm{syst.}))\%$$

Experimental search in K^- induced reactions

FINUDA at DAΦNE: $K^-_{stop} + X \rightarrow \Lambda + p + X'$

only back-to-back Λp pairs ($\cos\theta_{\Lambda p} < -0.8$)

detected particles

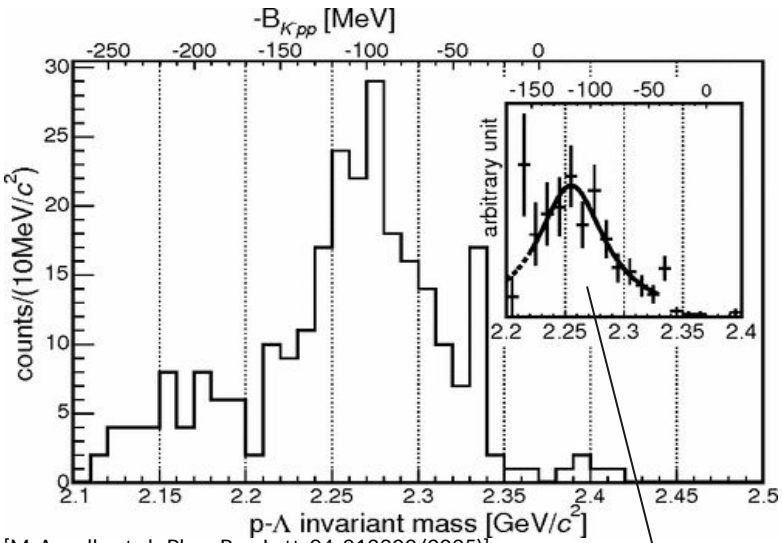

[M. Agnello et al., Phys. Rev. Lett. 94, 212303 (2005)]

Interpreted as the signal of:
$K^-pp \rightarrow \Lambda + p$

extracted parameters:

$BE = (115^{+6}_{-5}\,(stat.)^{+3}_{-4}\,(syst.))$ MeV

$\Gamma = (67^{+14}_{-11}(stat.)^{+2}_{-3}(syst.))$ MeV/c²

E549 at KEK: $K^-_{stop} + {}^4He \rightarrow \Lambda + p + X'$

detected particles

[T. Suzuki et al., Mod. Phys. Lett. A23 (2008) 2520-2523.]

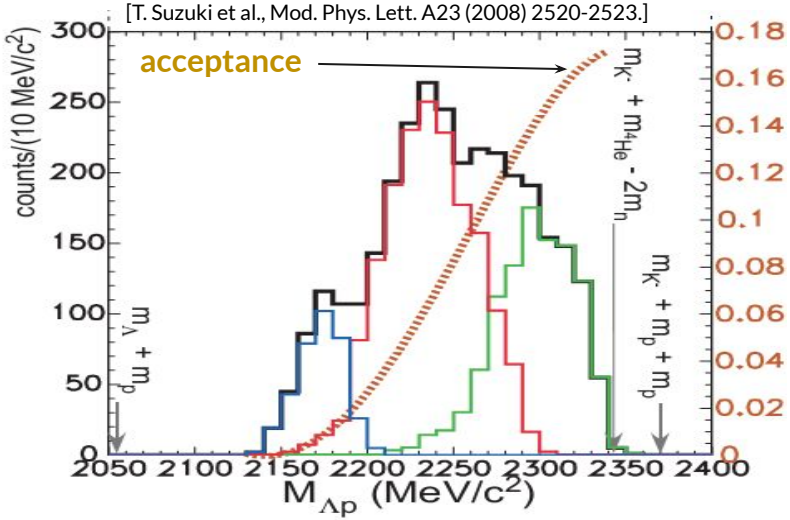

Using the missing mass information, three components to the invariant mass spectrum are found:

- **1NA**: K^- single nucleon absorption
- **2NA**: K^- two nucleon absorption
- **2NA + conversion**, **multi-nucleon**, or **Bound State**?

Λp analysis: K⁻ pp bound state

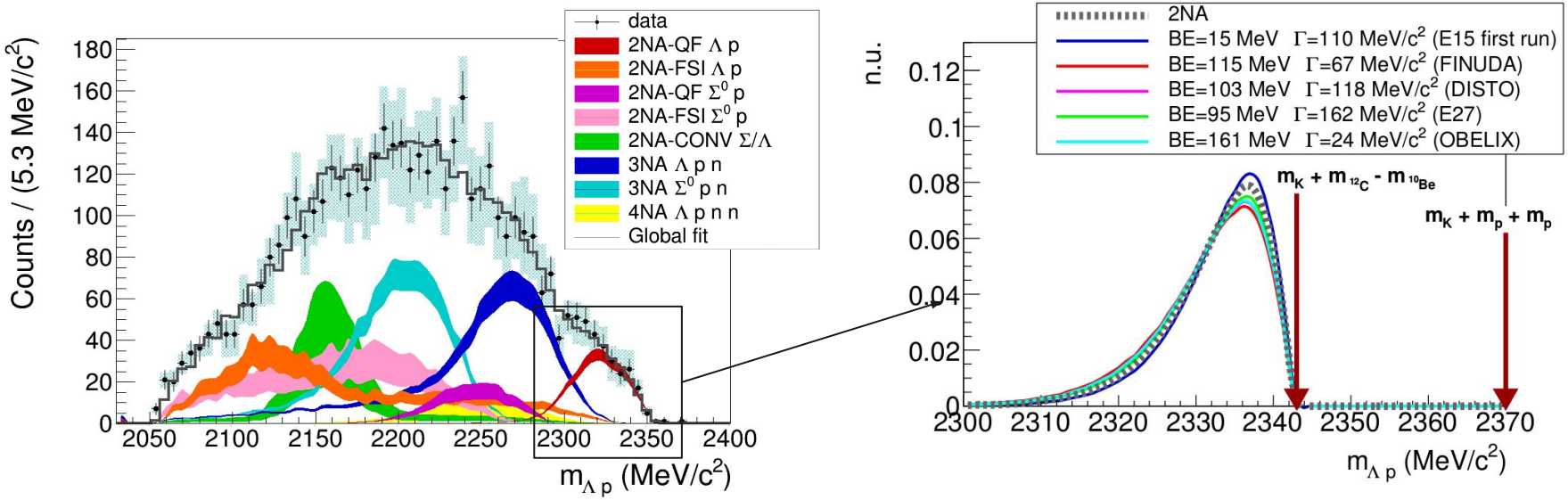

K⁻pp bound state contribution **completely overlaps** with the K⁻2NA

[R. Del Grande, K. Piscicchia, O. Vazquez Doce et al., Eur.Phys.J. C79 (2019) no.3, 190]
[R. Del Grande, K. Piscicchia, S. Wycech, Acta Phys. Pol. B 48 (2017) 1881]

Λp analysis: K⁻ pp bound state

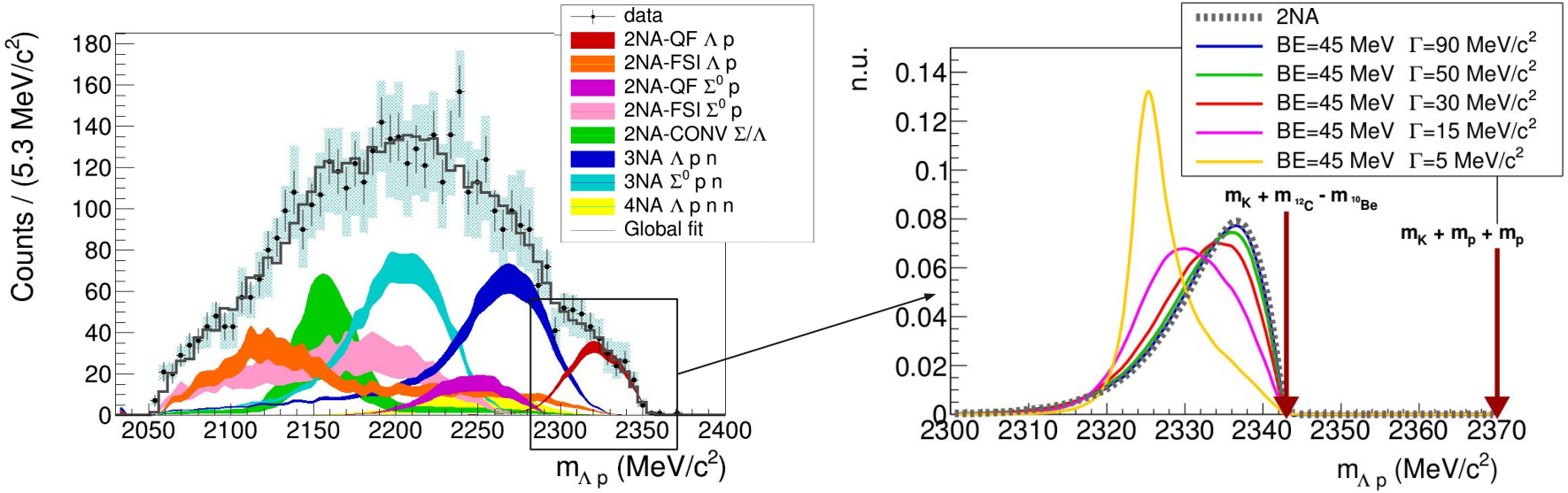

K⁻pp bound state contribution **completely overlaps** with the K⁻2NA

[R. Del Grande, K. Piscicchia, O. Vazquez Doce et al., Eur.Phys.J. C79 (2019) no.3, 190]
[R. Del Grande, K. Piscicchia, S. Wycech, Acta Phys. Pol. B 48 (2017) 1881]

Λp analysis: K^- pp bound state search

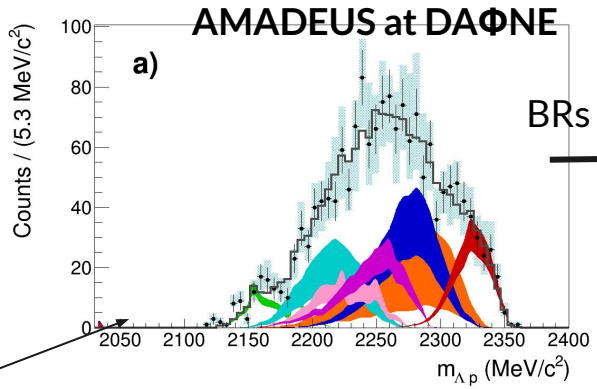

BRs evaluation

Process	Branching Ratio (%)
2NA-QF Λp	$0.20 \pm 0.04(\text{stat.}) \pm 0.02(\text{syst.})$
2NA-FSI Λp	$3.8 \pm 2.3(\text{stat.}) \pm 1.1(\text{syst.})$
2NA-QF Σ^0p	$0.54 \pm 0.20(\text{stat.})\ ^{+0.20}_{-0.16}(\text{syst.})$
2NA-FSI Σ^0p	$5.4 \pm 1.5(\text{stat.})\ ^{+1.0}_{-2.7}(\text{syst.})$
2NA-CONV Σ/Λ	$22 \pm 4(\text{stat.})\ ^{+1}_{-12}(\text{syst.})$
3NA Λpn	$1.1 \pm 0.3(\text{stat.}) \pm 0.2(\text{syst.})$
3NA Σ^0pn	$1.9 \pm 0.7(\text{stat.})\ ^{+0.8}_{-0.4}(\text{syst.})$

only **back-to-back Λp** pairs ($\cos\theta_{\Lambda p} < -0.8$)

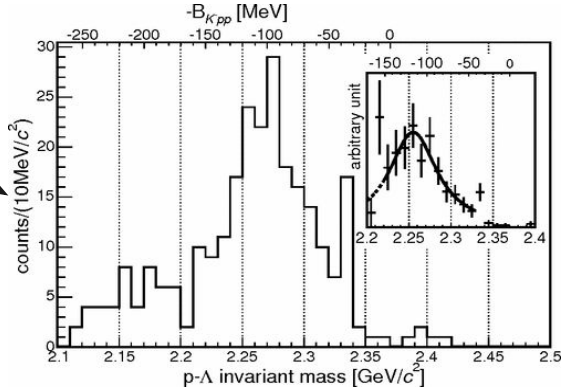

[M. Agnello et al., Phys. Rev. Lett. 94, 212303 (2005)]

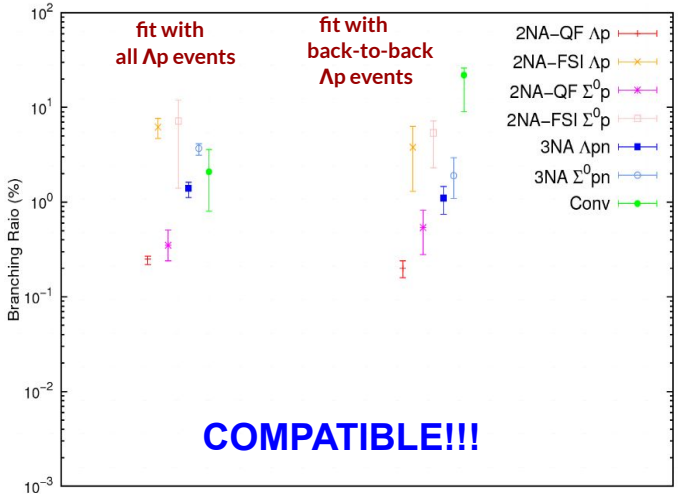

Λt analysis: Cross section and BR for 4NA

GOLDEN CHANNEL to extrapolate the K^- 4NA

$$K^- + \text{“ppnn”} \rightarrow \Lambda + t$$

Previous data:

- in ^{4}**He:** bubble chamber experiment

/M. Roosen, J. H. Wickens, Il Nuovo Cimento 66, 101 (1981)/

only **3 events** compatibile with Λt kinematics found

BR($K^{-4}He \rightarrow \Lambda t$) **= (3 ± 2) × 10^{-4} /K^-_{stop}** → **global, no 4NA**

- in **solid targets:** ^{6,7}**Li,** ^{9}**Be** (FINUDA)

/Phys. Lett. B, 229 (2008)/

40 events, only **back-to-back data**

Λt emission yield → $10^{-3} - 10^{-4}$ / K^-_{stop}

→ **global, no 4NA**

AMADEUS analysis

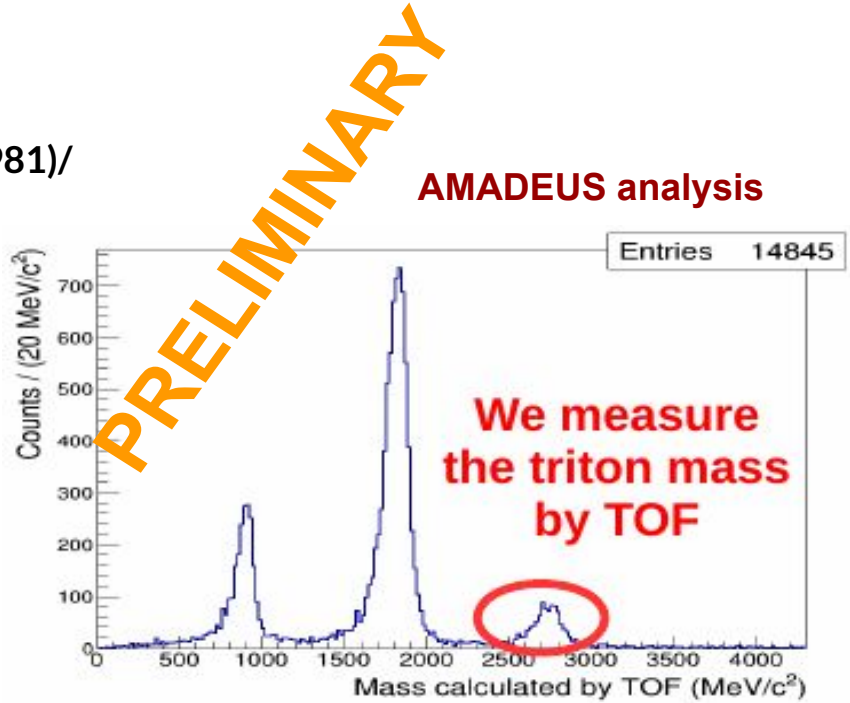

MC simulations: efficiency & resolution

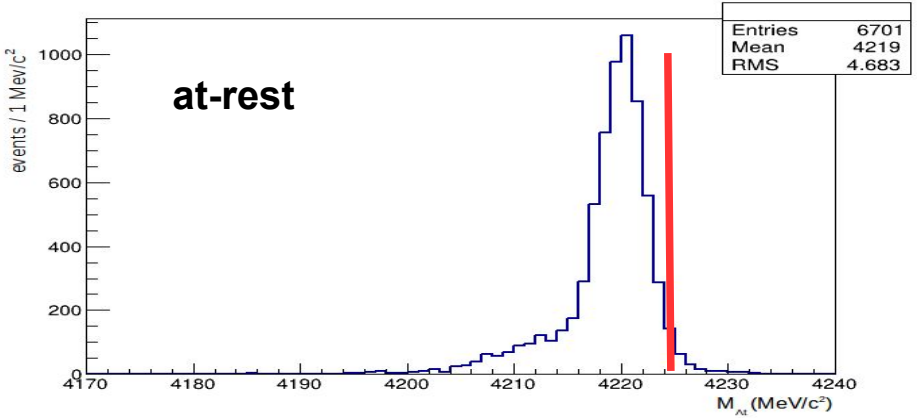

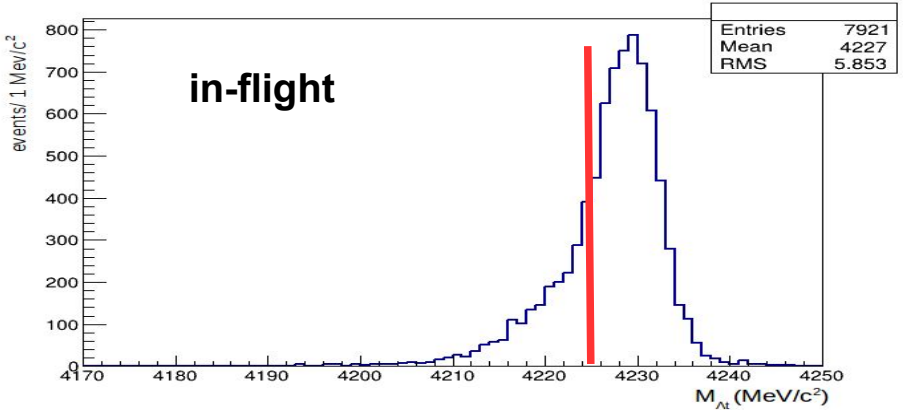

mass threshold at-rest

$M_{\Lambda t}$ invariant mass resolution = 2.2 MeV/c^2

overall <u>detection + reconstruction efficiency</u> for 4NA direct Λt production :

$$\epsilon_{4\mathrm{NA},ar,\Lambda t} = 0.0493 \pm 0.0006 \quad ; \quad \epsilon_{4\mathrm{NA},if,\Lambda t} = 0.0578 \pm 0.0006,$$

at-rest **in-flight**

Λt analysis: Cross section and BR for 4NA in **$K^{-}\,{}^{4}He \rightarrow \Lambda t$** process

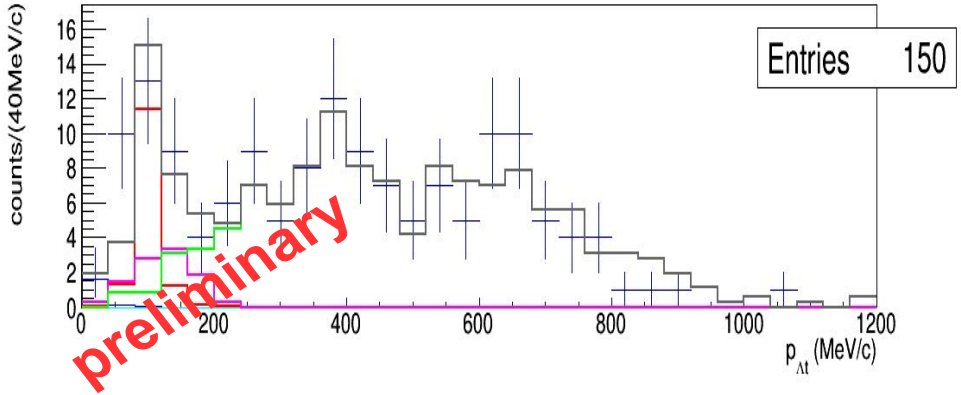

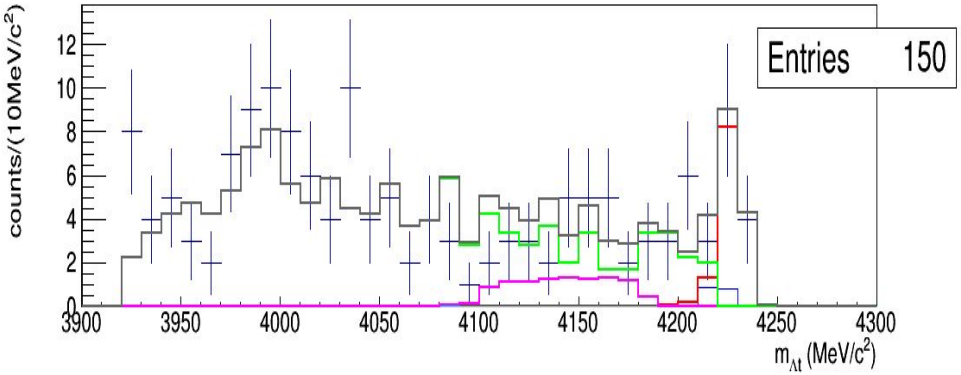

BR($K^{-4}He$(4NA) → Λt) **< 2.0 × 10^{-4} /K_{stop} (95% c. l.)**

σ(100 **± 19** MeV/c) ($K^{-4}He$(4NA) →Λt) =
= (0.81 ± 0.21 (stat) $^{+0.03}_{-0.04}$ (syst)) mb

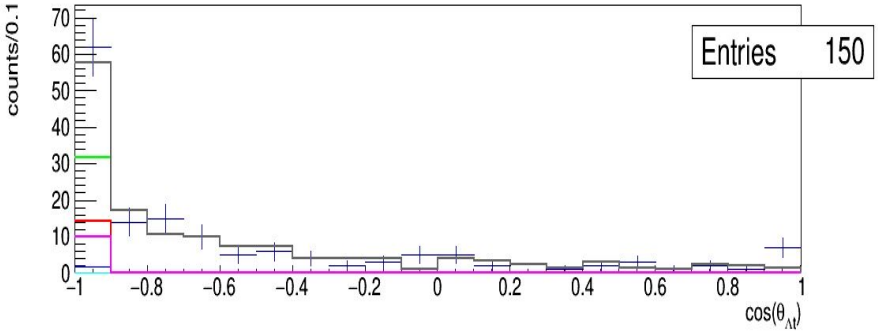

Λt analysis: Cross section and BR for 4NA in **$K^{-}\,{}^{4}He \rightarrow \Lambda t$** process

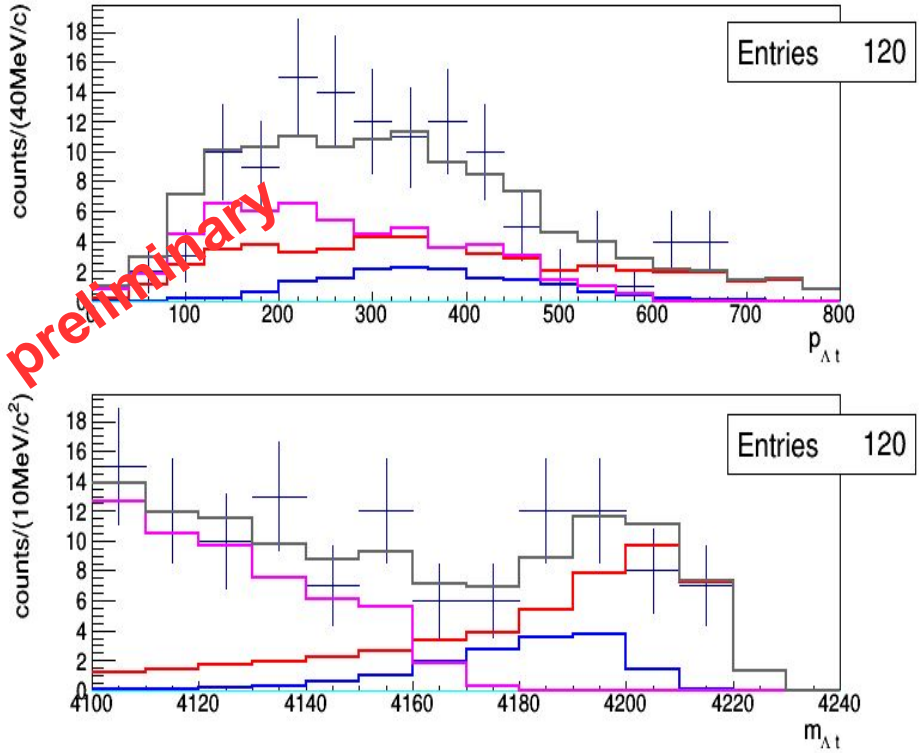

BR($K^{-12}C$(4NA) → Λt ^{8}Be) = **$1.5 \pm 0.5 \times 10^{-4}$ (stat) /K_{stop}**

σ($K^{-12}C$ (4NA) →Λt ^{8}Be) = **0.58 ± 0.11 (stat) mb**

σ($K^{-12}C$ (4NA) →Σ^{0}t ^{8}Be) = **1.88 ± 0.35 (stat) mb**

NEUTRON STARS - the Hyperon puzzle

Hyperons may appear in the inner n.s. core for 2-3 ϱ_0 → nucleons into hyperons conversion relieves Fermi pressure → softer EoS → less mass can be sustained

see e.g. S. Balberg, A. Gal, Nucl. Phys. A625 (1997) 435, L. Tolos, M. Centelles, A. Ramos, Astron. Soc. Austral. 34 (2017), D. Lonardoni, F. Pederiva, S. Gandolfi, Phys. Rev. C89 (1) (2014) 014314,. H. J. Schulze, A. Polls, A. Ramos, I. Vidana, Phys. Rev. C73 (2006), Wiktorowicz, G.; Drago, A.; Pagliara, G.; Popov, S.B.Astrophys. J. 2017, 846, 163.

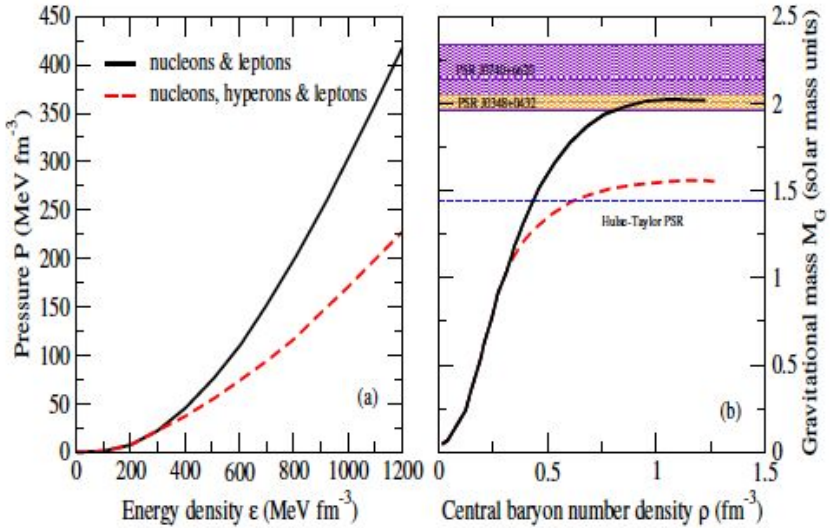

Especially in microscopic models the maximum reachable mass is not compatible with the 2 solar mass observations!

Figure from L. Tolos, L. Fabbietti, Progress in Particle and Nuclear Physics, Volume 112, 2020

Hyperon puzzle - Y-N, Y-Y interaction

possible way out stiff Y-N / Y-Y interaction explored in RMF models → vectors mesons exchange among baryons leads to a repulsive behaviour of the baryon-baryon interaction

see e.g. K. A. Maslov, E. E. Kolomeitsev, D. N. Voskresensky, Phys. Lett. B748 (2015), S. Weissenborn, D. Chatterjee, J. Schaner-Bielich, Phys. Rev. C85 (6) (2012)

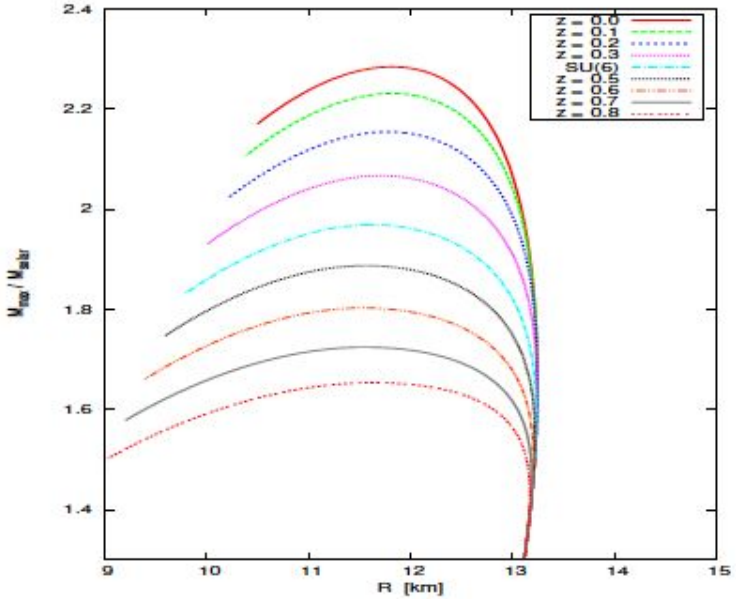

***z* parameter accounts for the singlet and octet meson coupling constants to baryons**

Hyperon puzzle - three body forces

The hyperonic three-body forces, as in the case of three-nucleon forces, might induce an additional repulsion at high densities so as to make the EoS stiff enough

strongly model dependent: see e.g. I. Vidana, D. Logoteta, C. Providencia, A. Polls, I. Bombaci, EPL 94 (1) (2011) (**Fig. left curves 1,2 nucleons only, curves 3,4 nucleons and hyperons**), D. Logoteta, I. Vidana, I. Bombaci, Eur. Phys. J. A55 (11) (2019) (**Fig. right dashed dotted lines with 3BF NNΛ reaches 2Sol Mass**), D. Lonardoni, A. Lovato, S. Gandolfi, F. Pederiva, Phys. Rev. Lett. 114 (9) (2015)

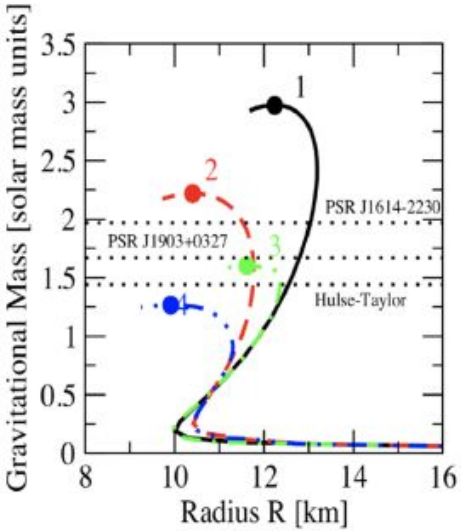

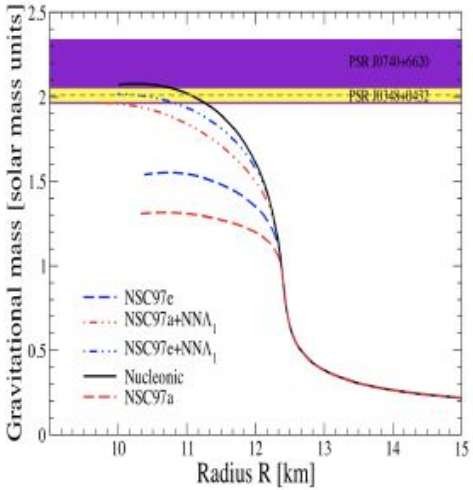

Y-N experimental information from scattering experiments

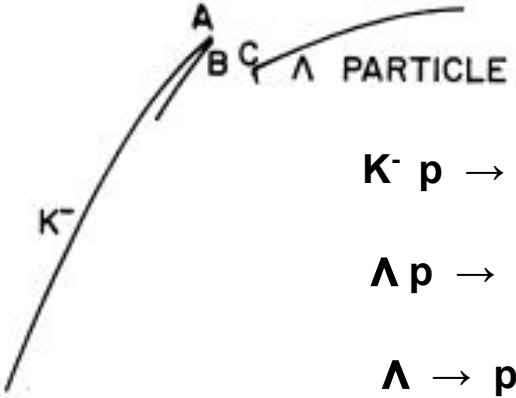

$K^- p \rightarrow \Lambda n$

$\Lambda p \rightarrow \Lambda p$

$\Lambda \rightarrow p \pi^-$

- Hydrogen bubble chamber exposed to a secondary K- beam.
- The stopped K- particle and the resulting charged products identified looking at the recorded photographs of the bubble chamber reactions.
- The following scattering of hyperons on protons and their weak decays are then tagged.

Phys. Lett. B37 (1971) 204-206.
Phys. Rev. 173 (1968) 1452-1460.
Phys. Rev. 175 (1968) 1735-1740.

J-PARC E40 aims to measure the differential cross sections of: Σ± p elastic scatterings, Σ−p → Λn conversion, by means of the reaction $p(\pi^{\pm}, K^{+})\Sigma^{\pm}$ using LH_2 target

No experimental information on Σ^0-N/NN and in general on Y-NN interaction from scattering experiments

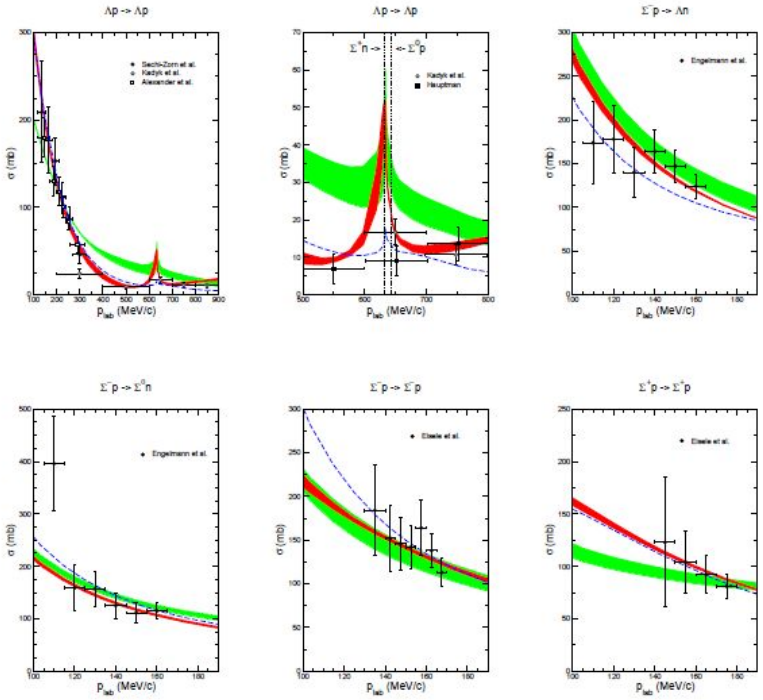

Figure 2: "Total" cross section σ (as defined in Eq. (24)) as a function of $p_{\rm lab}$. The experimental cross sections are taken from Refs. [52] (filled circles), [53] (open squares), [65] (open circles), and [66] (filled squares) ($\Lambda p \to \Lambda p$), from [54] ($\Sigma^- p \to \Lambda n$, $\Sigma^- p \to \Sigma^0 n$) and from [55] ($\Sigma^- p \to \Sigma^- p$, $\Sigma^+ p \to \Sigma^+ p$). The red/dark band shows the chiral EFT results to NLO for variations of the cutoff in the range $\Lambda = 500, \ldots, 650$ MeV, while the green/light band are results to LO for $\Lambda = 550, \ldots, 700$ MeV. The dashed curve is the result of the Jülich '04 meson-exchange potential [36].

See e.g. Nucl. Phys. A 915 (2013) 24-58
Eur. Phys. J. A 51, 53 (2015),

and talk U. G. Meißner
for a discussion on hypernuclei physics

Σ^0-p & Λ-Λ by femtoscopy technique

Measurement of the correlation in the momentum space for (Y-p) (Y-Y) pairs exploiting the femtoscopy technique, a correlation function due to the background computed as baseline for Σ^0-p.

arXiv:1910.14407.
S. Acharya, et al., Phys. Lett. B797 (2019)

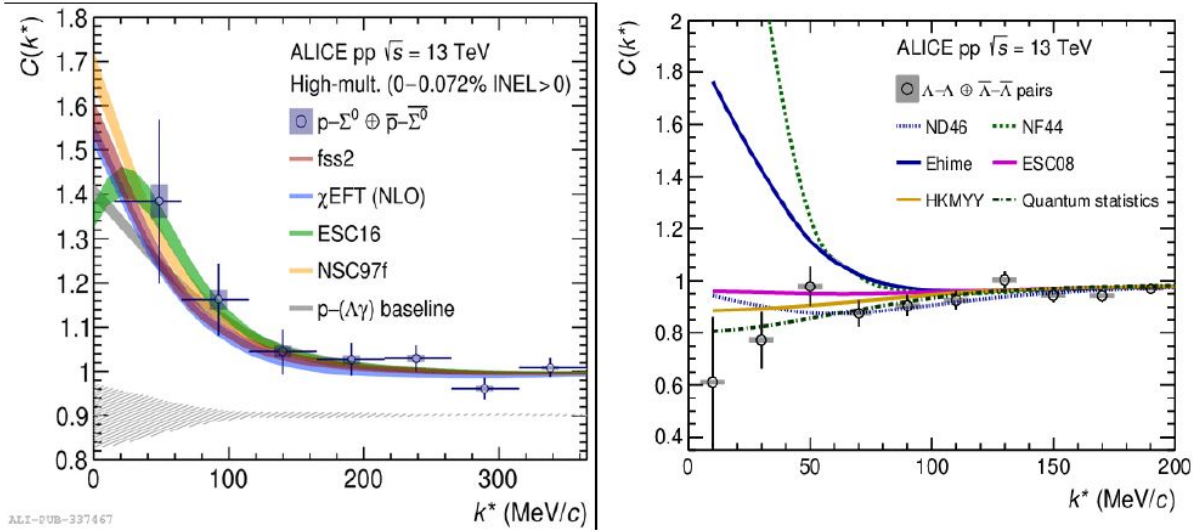

Figure 31: *(Color online)* Left panel: $p\Sigma^0$ correlation function measured in pp collisions at $\sqrt{s} = 13$ TeV at the LHC by the ALICE collaboration [200]. Right panel: $\Lambda\Lambda$ correlation measured in pp collisions at $\sqrt{s} = 13$ TeV at the LHC by the ALICE collaboration [202].

Figure from L. Tolos, L. Fabbietti, Progress in Particle and Nuclear Physics, Volume 112, 2020

$$(K^- \ ppn) + n \rightarrow \Sigma^0 \ d + n$$

3NA in ^{4}He

for the investigation of the

Σ^0-N & Σ^0-(NN) interaction

Involved reactions:

3NA - $(K^- ppn) + n \rightarrow \Sigma^0 d + n$

- The Σ^0 identification (with respect to Λ) enables to avoid the internal conversion background. Moreover there is presently no available Σ^0-N scattering data.

- ^{4}He target $\rightarrow$ no nuclear fragmentation can follow the 3NA primary process.

+

3NA can be followed by two possible elastic FSI

1) n d $\rightarrow$ n d we may take advantage of the well known σNN data

2) Σ^0 n/d $\rightarrow$ Σ^0 n/d from which to extract information on Σ^0-N , Σ^0-(NN) interaction.

Involved reactions - signal:

3NA - $(K^- ppn) + n \rightarrow \Sigma^0 d + n$

- We show that the most energetic part of the $m_{\Sigma 0d}$ invariant mass spectrum is correlated to high

  $p_{\Sigma 0}$ and p_d momenta, this corresponds to the 3NA - $(K^- ppn)$ process.

The Σ^0 d statistics from K- captures in the gas filling the KLOE DC is poor. Moreover K- in ^{12}C (from isobutane) are not distinguishable from K- captures on ^4He.

A dedicated measurement with pure ^4He target (^3He target also helpful for comparison) is mandatory for this purpose.

3NA

$(K^- ppn) + n \rightarrow \Sigma^0 d + n$

without FSI

Corresponds to the highest part of the invariant mass spectrum

the blue region is populated by free 3NA,

at slightly lower energy is the 3NA followed by 2B & 3B FSI.

Our aim is to measure the relative contributions of the two processes.

At lower energies 2NA is involved and complex FSI processes with fragmentation of the residual ^{8}Be (not present in ^{4}He target).

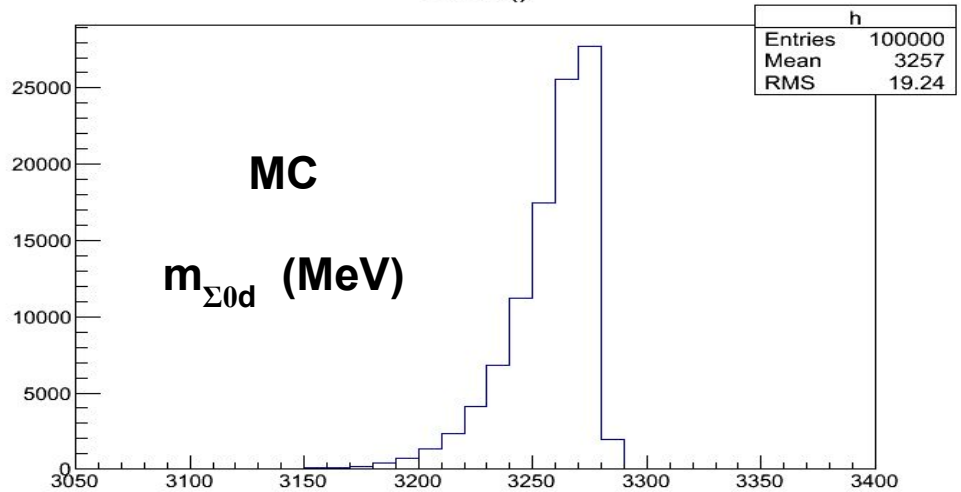

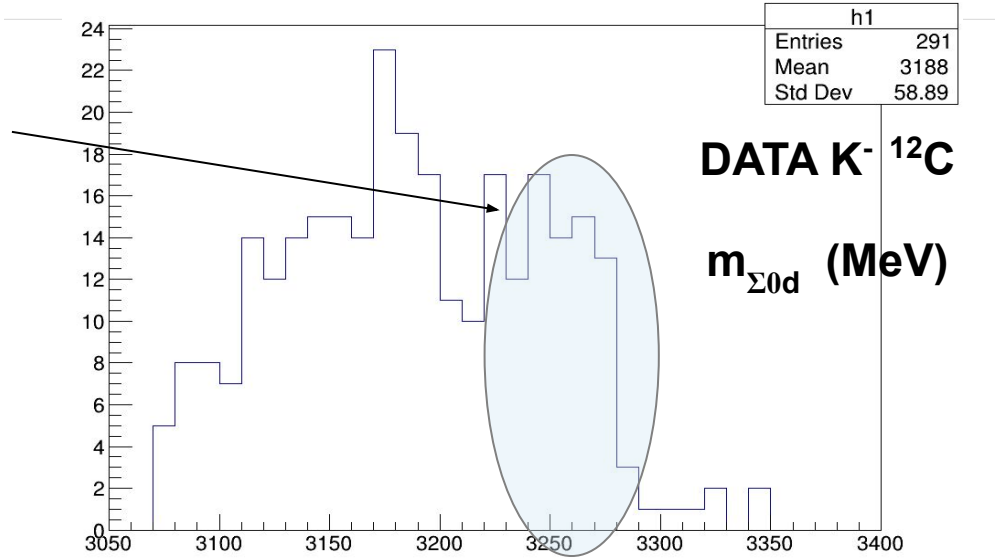

3NA

$(K^- ppn) + n \rightarrow \Sigma^0 d + n$

without FSI

Corresponds to the highest part of the Σ^0 momentum spectrum.

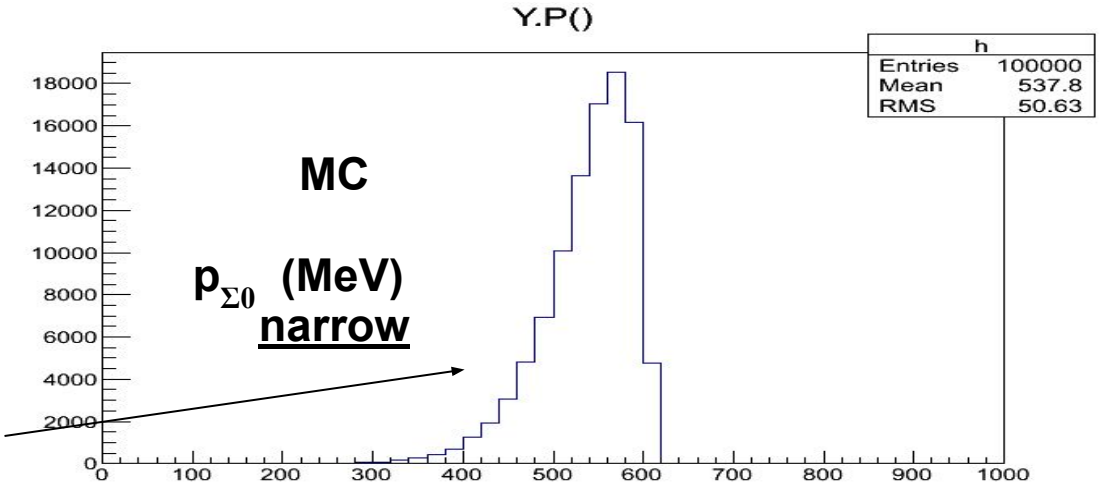

The narrow Σ^0 momentum distribution will enable to measure Σ^0-N and Σ^0-NN cross section at 550 ± 50 MeV/c.

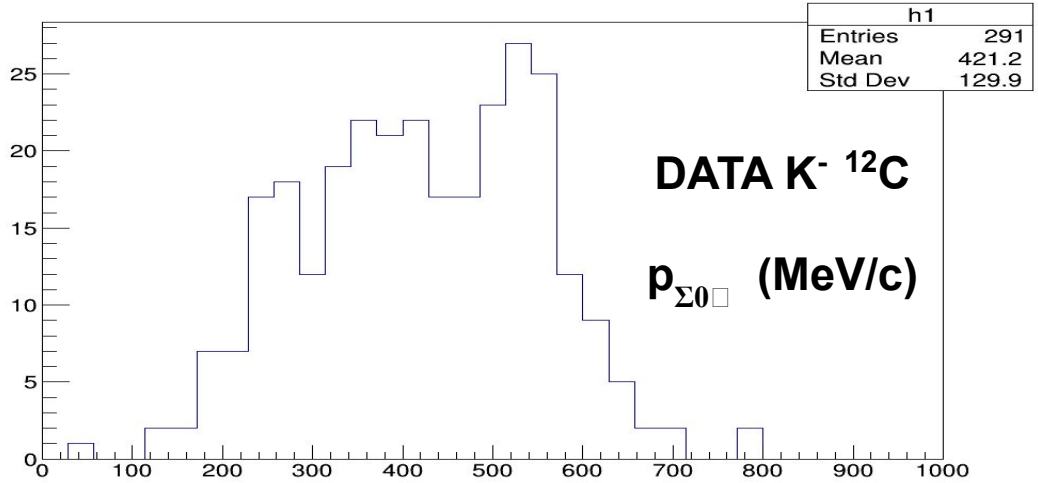

3NA $(K^- ppn) + n \rightarrow \Sigma^0 d + n$ wo FSI

- clean mometum mass correlation

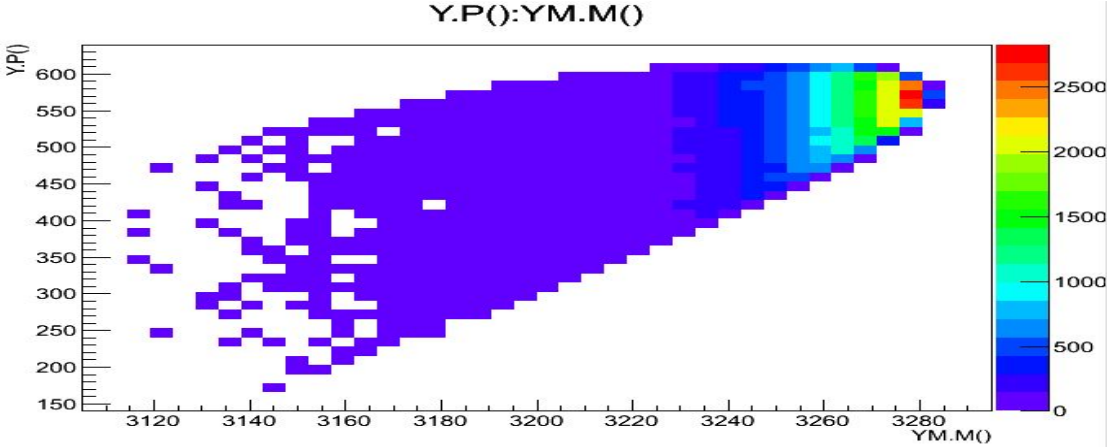

MC

$p_{\Sigma 0}$ vs $m_{\Sigma 0d}$

DATA K^- ^{12}C

$p_{\Sigma 0}$ vs $m_{\Sigma 0d}$

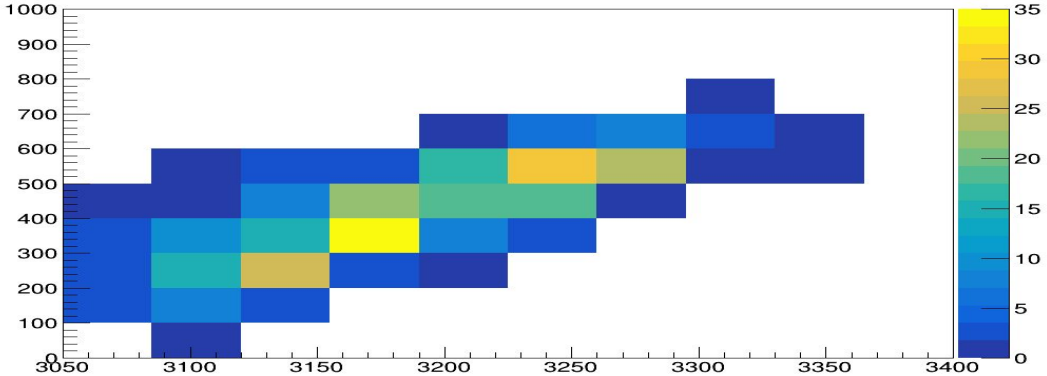

3NA - (K- ppn) + n → Σ0 d + n signature:

Highest Σ0 - d angular correlation - low Fermi momentum neutron

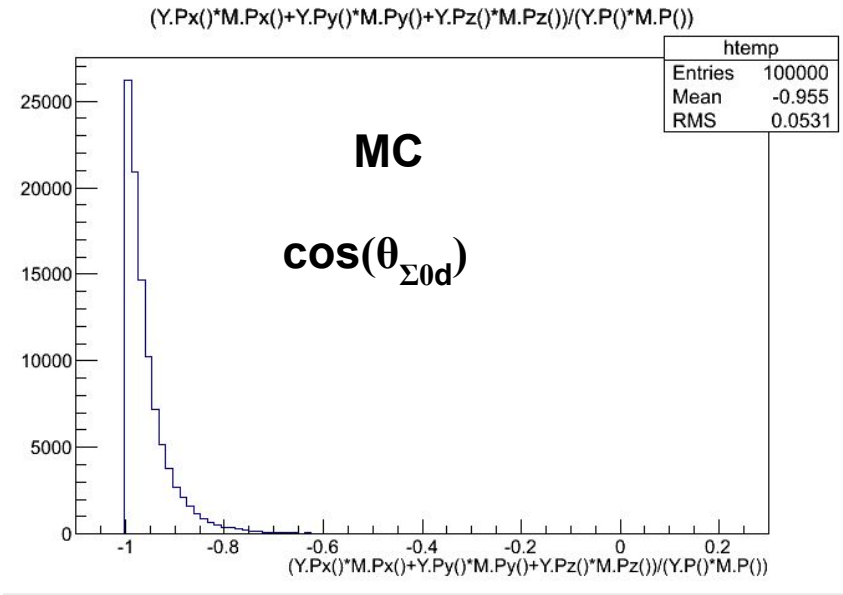

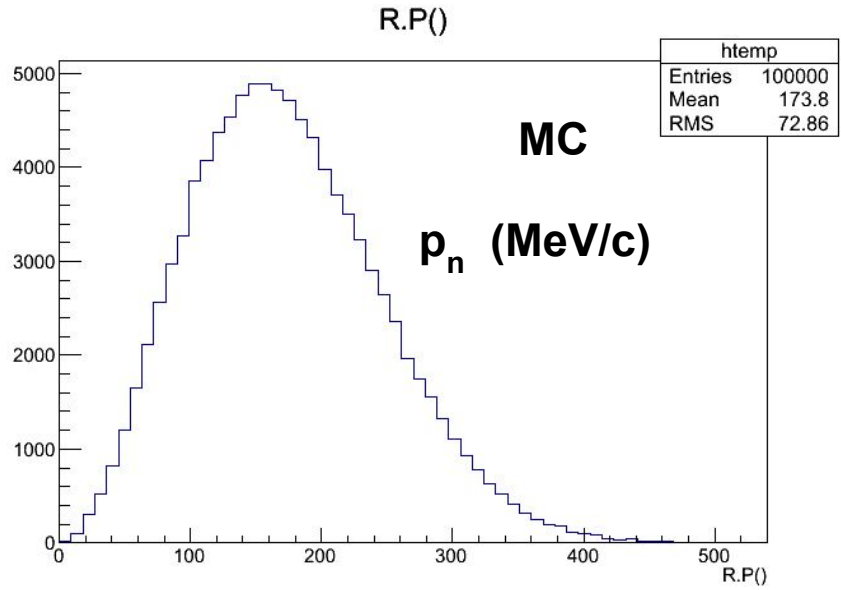

Involved reactions - background:

2NA - $(K^- pn) + d \rightarrow \Sigma^0 n + d$

+

2 possible elastic FSI

1) $n\,d \rightarrow n\,d$ we may take advantage of the well known σ_{NN} data

2) $\Sigma^0\,d/n \rightarrow \Sigma^0\,d/n$ ***well separated in the lower energy part of the final state phase space***

2NA

- (K- pn) + d → Σ0 n + d
- lower invariant mass

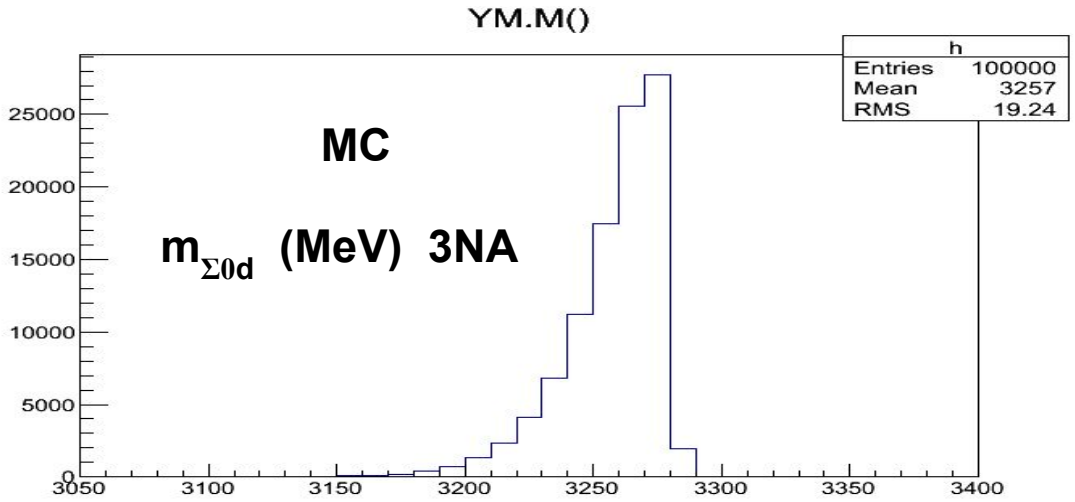

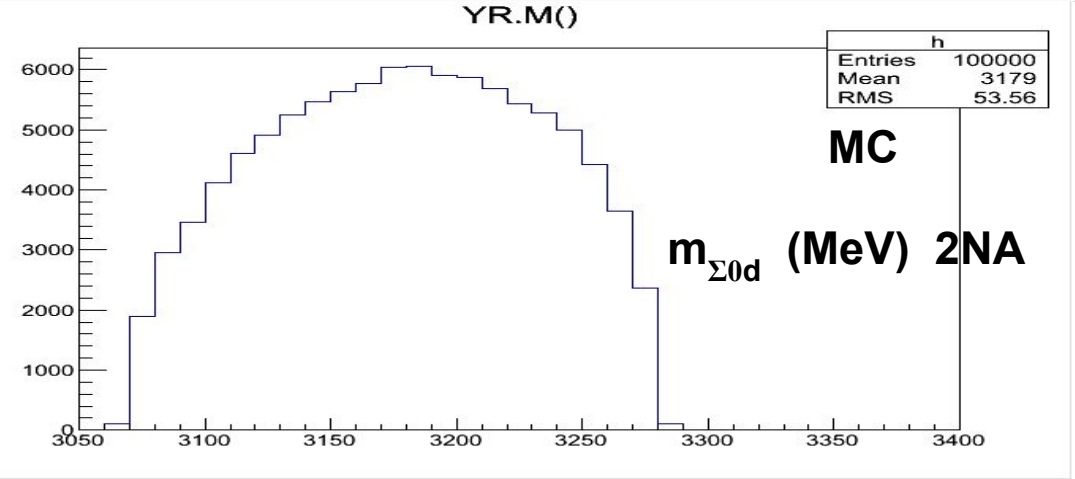

2NA

- (K- pn) + d → Σ0 n + d
- high momentum neutrons

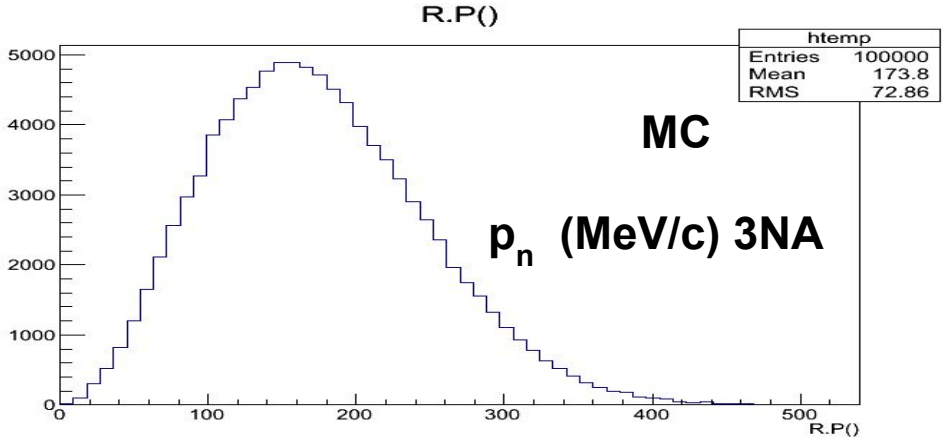

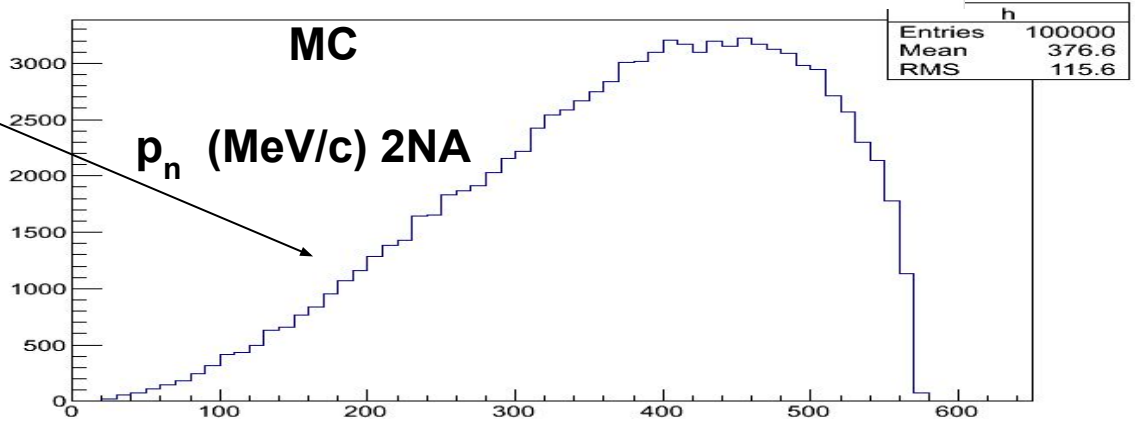

Detection of neutrons will be crucial for a clean separation of 3NA with respect to 2NA.

Involved reactions - background:

1NA - $(K^- p) + pnn \rightarrow \Sigma^0 \pi^0 n d$

$(K^- n) + ppn \rightarrow \Sigma^0 \pi^- p d$

- low energy (took away by the pion) not correlated Σ^0 d pairs. It is easy to be disentangled (similar to the Σ^0 p analysis).

Accurate model of the:

$$(K^- \ ppn) + n \rightarrow \Sigma^0 \ d + n$$

3NA in ^{4}He

+

$$\Sigma^0 \ d/n \rightarrow \Sigma^0 \ d/n \quad \text{FSI}$$

is needed to extract the corresponding cross sections from the measured shapes.

Ideal detector system for the proposed measurement is the combination of KN1 and KN2 experiments proposed by our collaboration:

- The kaon monitor: plastic scintillator pads read out on both sides with Silicon Photo-Multipliers, arranged around the interaction region, covering the TPC kaon entrance window
- active GEM-TPC: filled with very pure light gases (hydrogen, deuterium, helium-3, helium-4)
- charged kaon detector: made of plastic scintillator pads, read out with SiPMs, covering the outer part of the TPC window completely
- lead plates separated by a liquid scintillator: for detection of neutral particles.

see the talk by J. Zmeskal for details

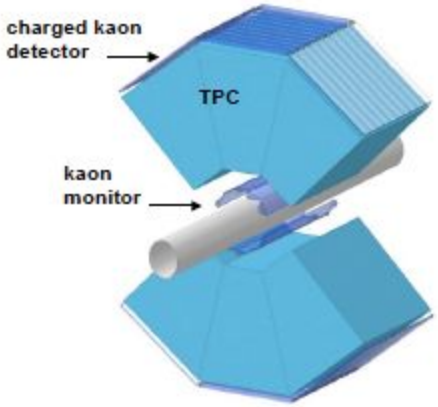

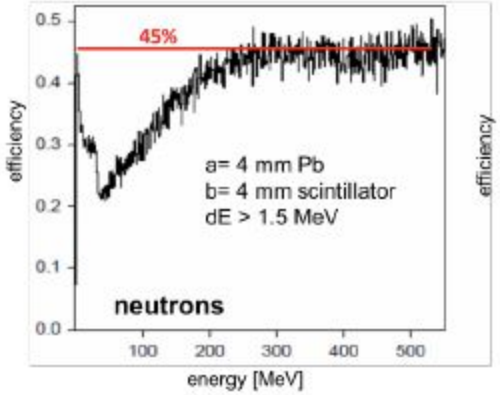

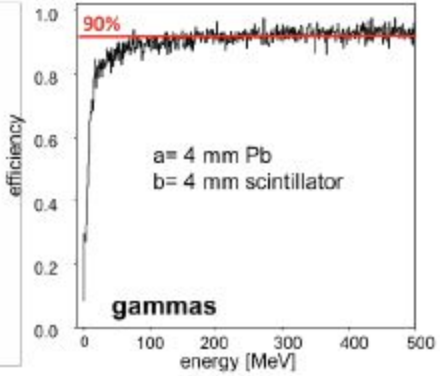

K^-p scattering amplitude

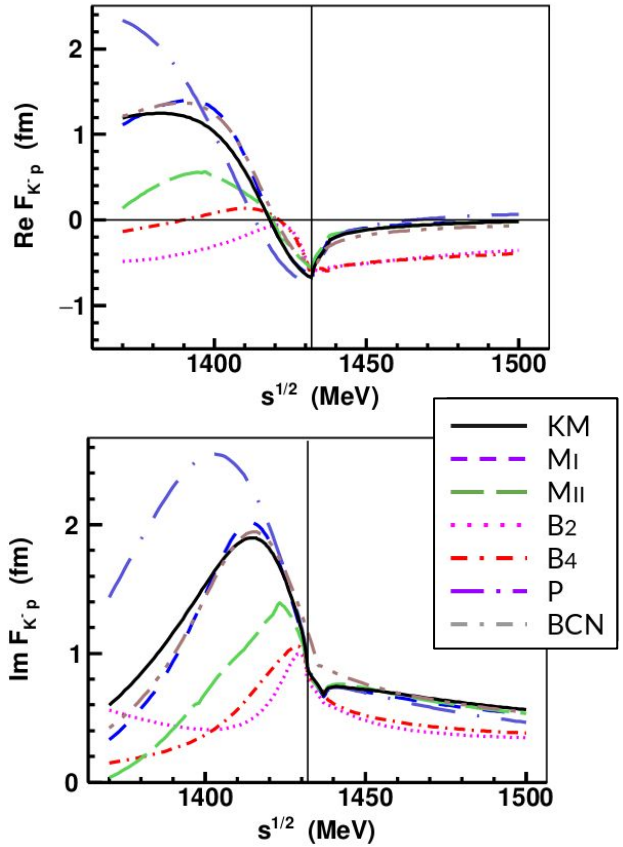

[from A. Cieply talk at MENU2019 conference]

K^-p scattering amplitude in Chiral calculations

- Kyoto-Munich (KM)
  Y. Ikeda, T. Hyodo, W. Weise, Nucl. Phys. A 881 (2012) 98
- Murcia (M_I , M_{II})
  Z. H. Guo, J. A. Oller, Phys. Rev. C 87 (2013) 035202
- Bonn (B_2 , B_4)
  M. Mai, U.-G. Meißner - Eur. Phys. J. A 51 (2015) 30
- Prague (P)
  A. Cieply, J. Smejkal, Nucl. Phys. A 881 (2012) 115
- Barcelona (BCN)
  A. Feijoo, V. Magas, À. Ramos, Phys. Rev. C 99 (2019) 035211

Experimental constraints at K̄N threshold

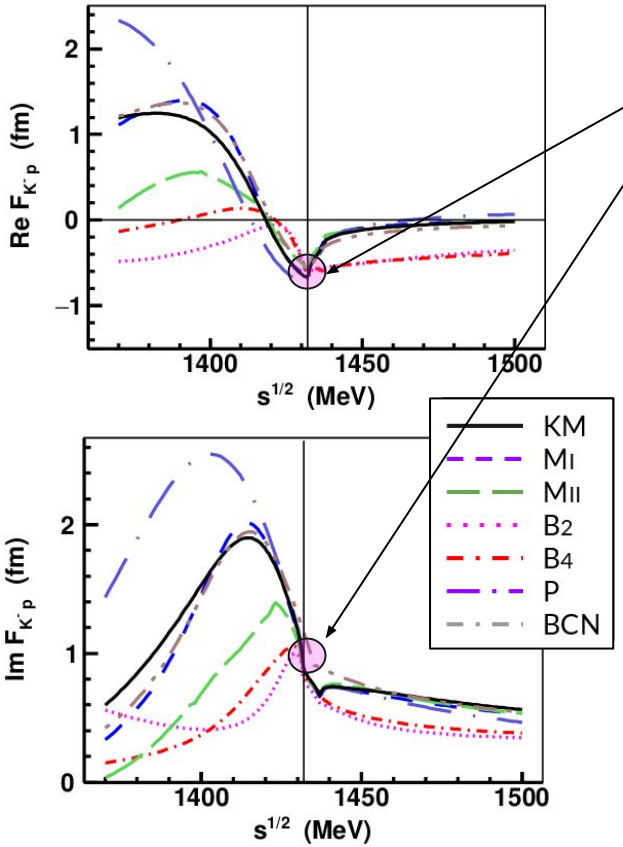

Precise SIDDHARTA measurement of kaonic hydrogen 1s level shift and width

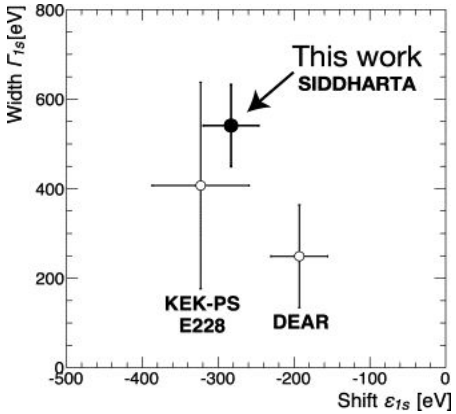

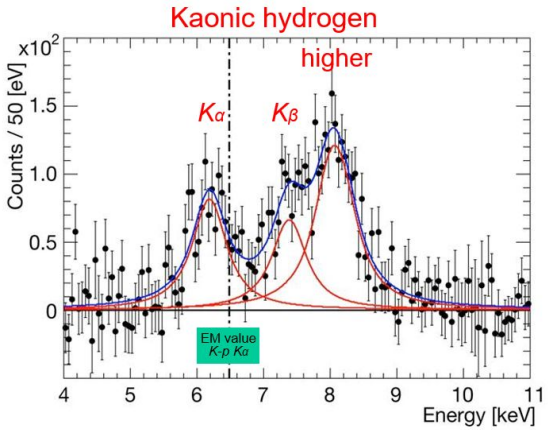

M. Bazzi et al.. 2011. (SIDDHARTA Coll.), Phys. Lett. B704, 113

$$\Delta E_N(1s) = 283 \pm 36(stat.) \pm 6(syst.)\ \text{eV}$$

$$\Gamma(1s) = 541 \pm 89(stat.) \pm 22(syst.)\ \text{eV}$$

$$\varepsilon + \frac{i\Gamma}{2} = 2\alpha^3\mu^2 a_{K^-p} = 412\,\frac{eV}{fm}\, a_{K^-p}$$

K^-p scattering amplitude

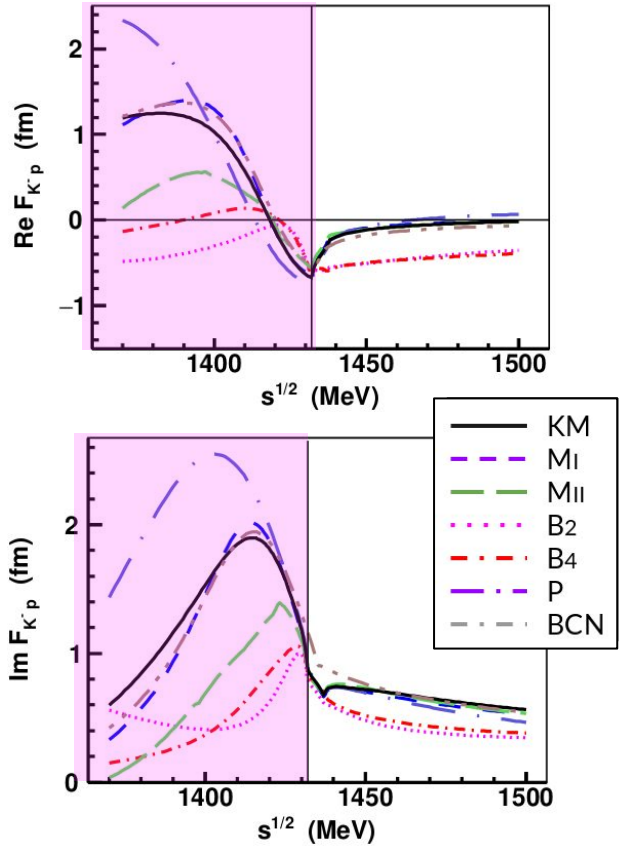

[from A. Cieply talk at MENU2019 conference]

K^-p scattering amplitude in Chiral calculations

- Kyoto-Munich (KM)
  Y. Ikeda, T. Hyodo, W. Weise, Nucl. Phys. A 881 (2012) 98
- Murcia (M_I , M_{II})
  Z. H. Guo, J. A. Oller, Phys. Rev. C 87 (2013) 035202
- Bonn (B_2 , B_4)
  M. Mai, U.-G. Meißner - Eur. Phys. J. A 51 (2015) 30
- Prague (P)
  A. Cieply, J. Smejkal, Nucl. Phys. A 881 (2012) 115
- Barcelona (BCN)
  A. Feijoo, V. Magas, À. Ramos, Phys. Rev. C 99 (2019) 035211

Large discrepancies in the region below threshold!

What above the threshold?

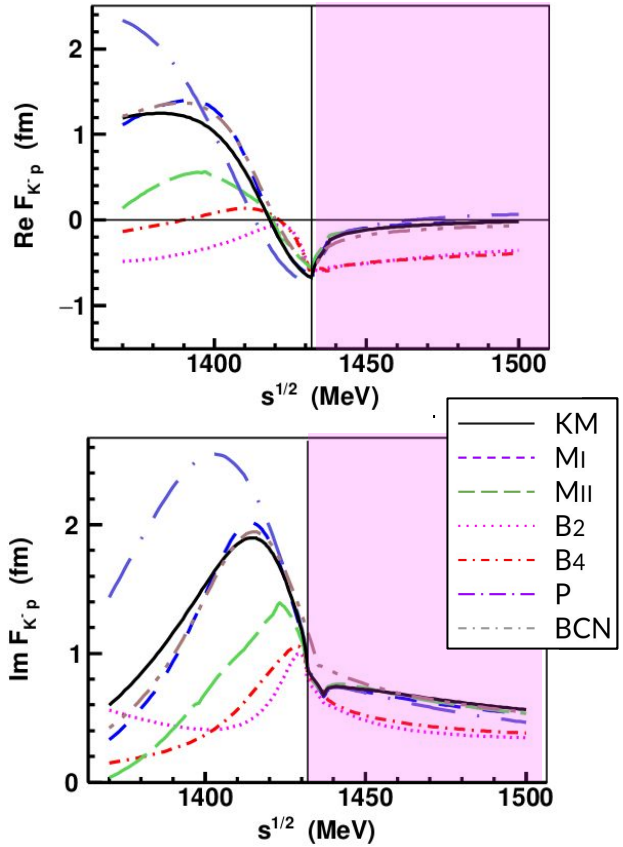

[from A. Cieply talk at MENU2019 conference]

K-p elastic and inelastic low-energy cross sections

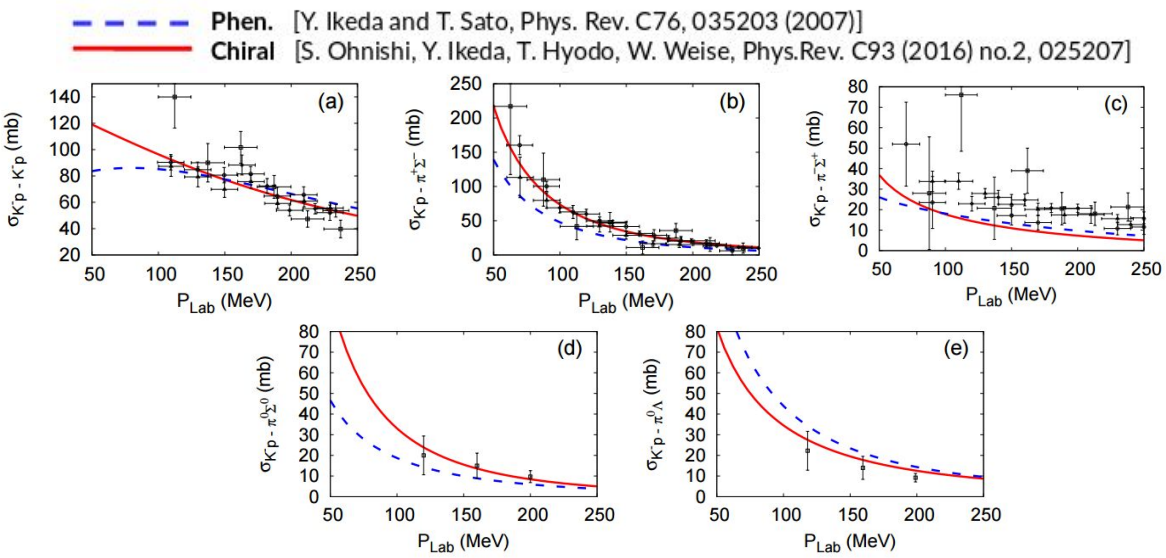

What above the threshold?

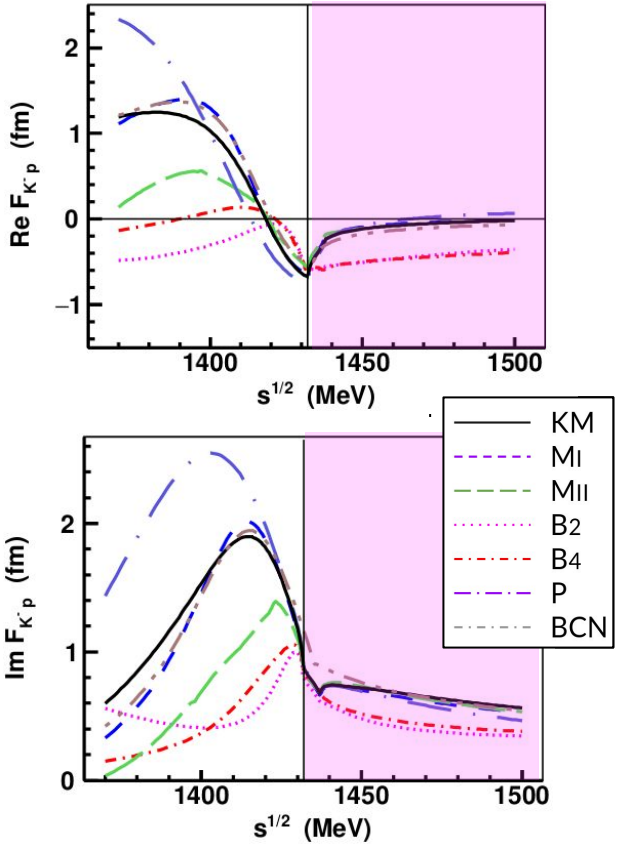

[from A. Cieply talk at MENU2019 conference]

K-p elastic and inelastic low-energy cross sections

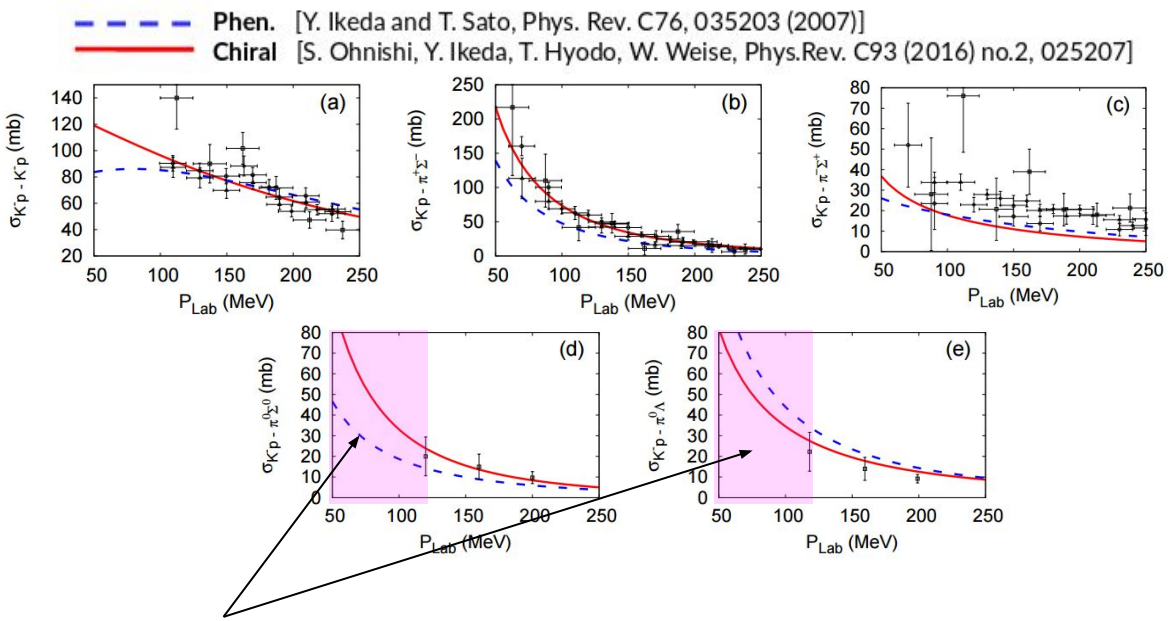

lack of data for $p_K < 120$ MeV/c ⟶ see the talk by J. Zmeskal for KN1 & KN2 proposals

K⁻n scattering amplitude

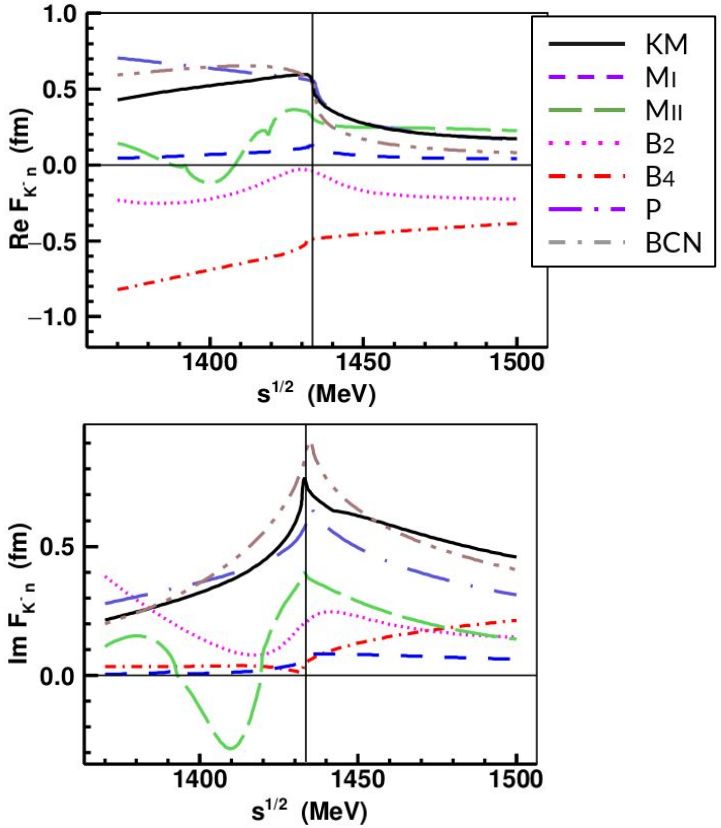

[from A. Cieply talk at MENU2019 conference]

K⁻n scattering amplitude (s-wave .. non resonant) in chiral calculations

<u>Even larger spread in I=1 channel</u>

Experimental information is missing:

- **SIDDHARTA-2 → first experimental constraint at threshold**
- **AMADEUS → first experimental constraint below threshold**

Experimental constraints below threshold

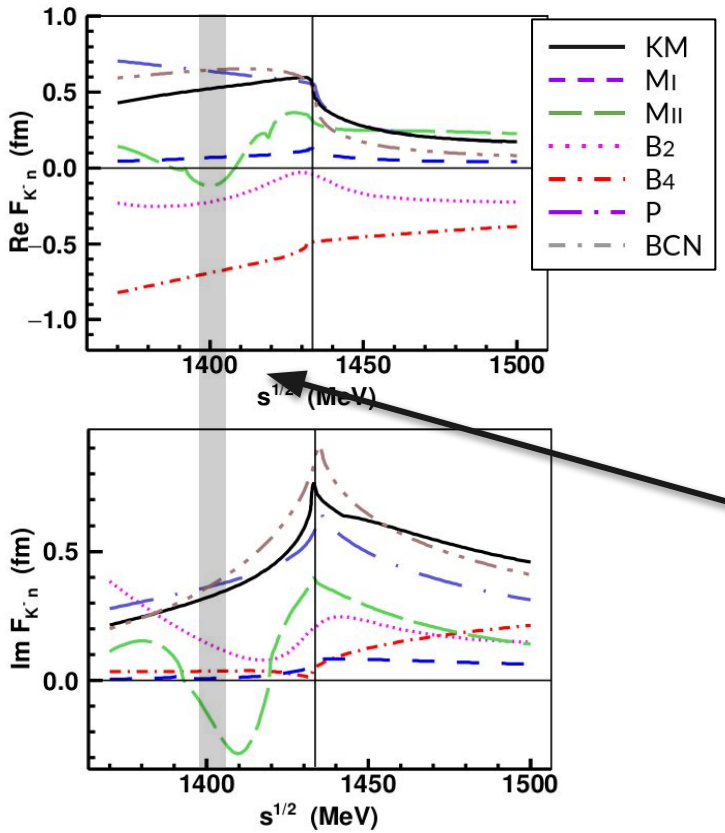

K^-n scattering amplitude with Chiral models

Large spread in I=1 channel

Experimental information is totally missing:

- **SIDDHARTA-2 → first experimental constraint at threshold**

- **AMADEUS → First determination of the non-resonant (s-wave) transition amplitude below threshold**

Investigated using:

K^- "n" → $\Lambda\pi^-$ to extract $|f^{N-R}_{\Lambda\pi}(I=1)|$

with bound neutron in ^{4}He

K- p → Λπ⁻ events selection and interpretation

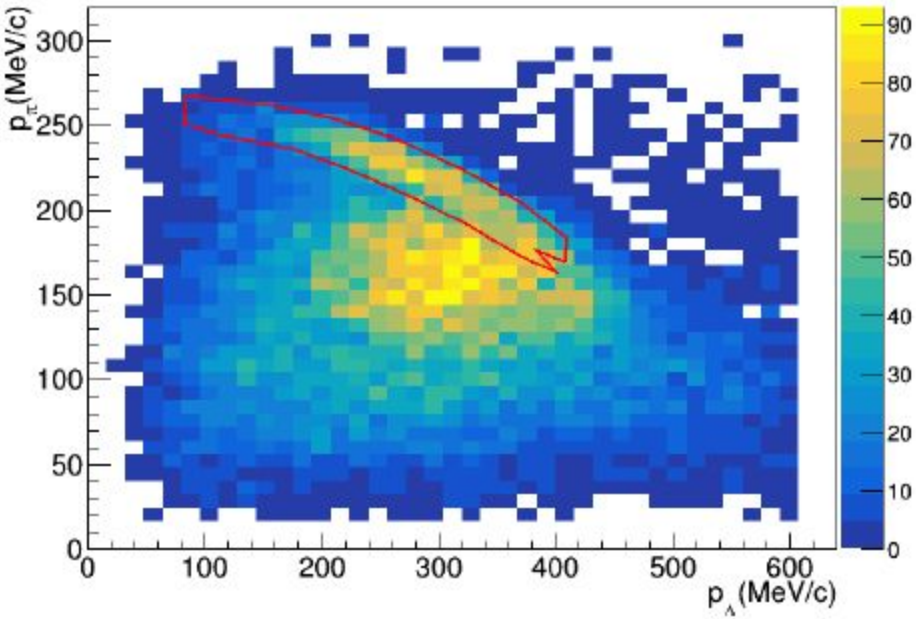

FIG. 2. *(Color online) Experimental distribution of the π^- vs Λ momenta. The red line represents the selection of the direct $\Lambda\pi^-$ production events. See the text for details.*

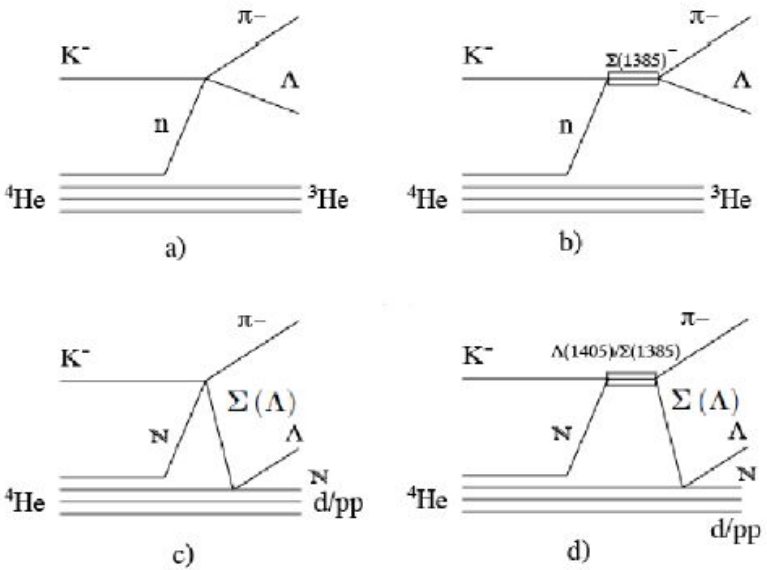

FIG. 1. *Panels a) and b) show the non-resonant and resonant $\Lambda\pi^-$ direct productions, respectively. Panels c) and d) show the primary hyperon-pion formation, followed by the inelastic/elastic scattering of the Σ/Λ hyperon on a single nucleon, for the resonant and non-resonant cases, respectively.*

Simultaneous fit : $p_{\Lambda\pi-}$ - $m_{\Lambda\pi-}$ - $\cos\theta_{\Lambda\pi-}$

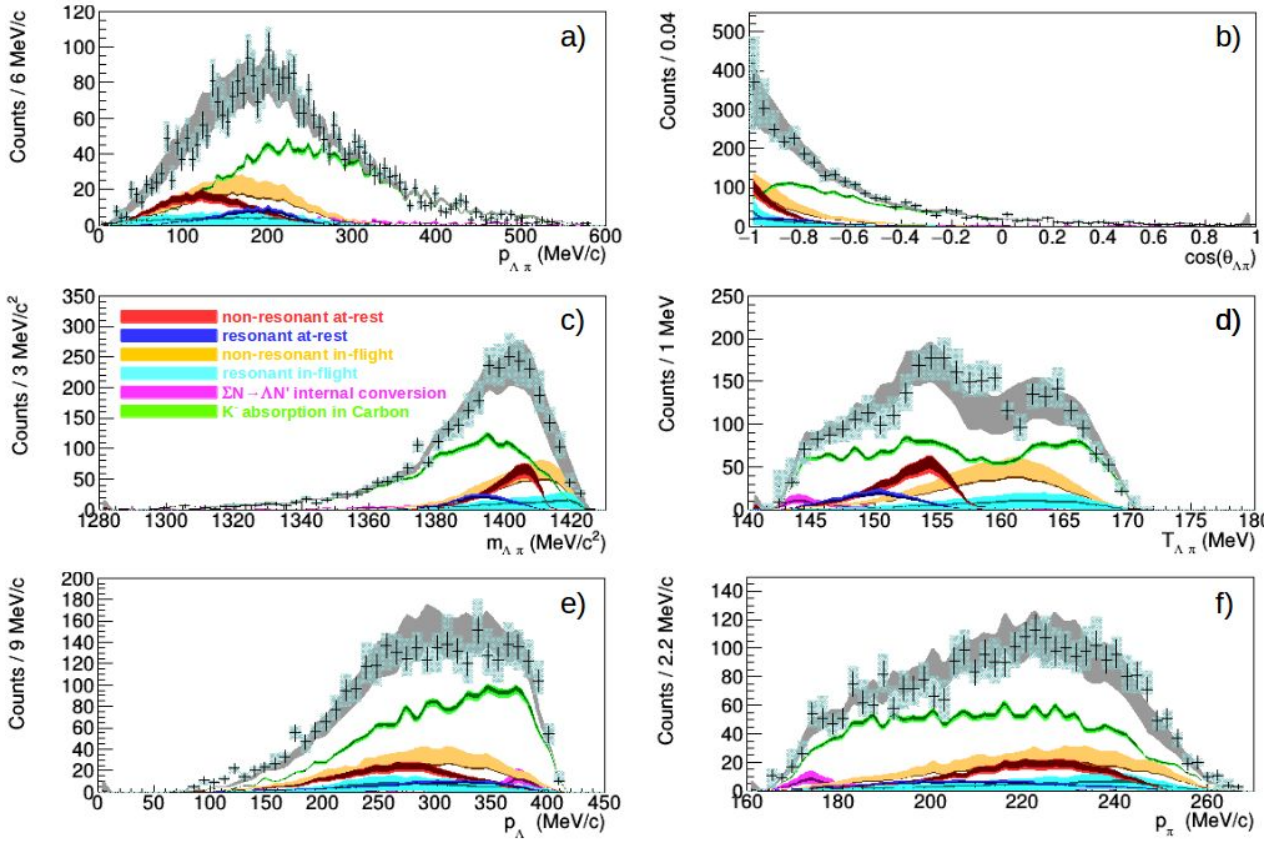

Investigated using:

K^- "n" ^{3}He → Λπ$^-$ ^{3}He

$$E_{\mathrm{Kn}} \sim -B_n - < \frac{p^2_{\Lambda\pi}}{2\mu_{\pi,\Lambda,3\mathrm{He}}} >$$

33 ± 6 MeV below threshold

see also

A. Cieply et al., Phys. Lett. B 702 (2011) 402
T. Hoshino et al., Phys. Rev. C 96 (2017) 045204
N. Barnea, E. Friedman,
A. Gal, Nucl. Phys. A968 (2017)

[K. Piscicchia, S. Wycech, L. Fabbietti et al. Phys.Lett. B782 (2018) 339-345]
[K. Piscicchia, S. Wycech, C. Curceanu, Nucl. Phys. A 954 (2016) 75-93]

Outcome of the measurement

Investigated using:

K^- "n" ^{3}He → Λπ$^-$ ^{3}He

Energy of the K^-n system:

$$E_{\mathrm{Kn}} \sim -B_n - < \frac{p^2_{\Lambda\pi}}{2\mu_{\pi,\Lambda,3\mathrm{He}}} >$$

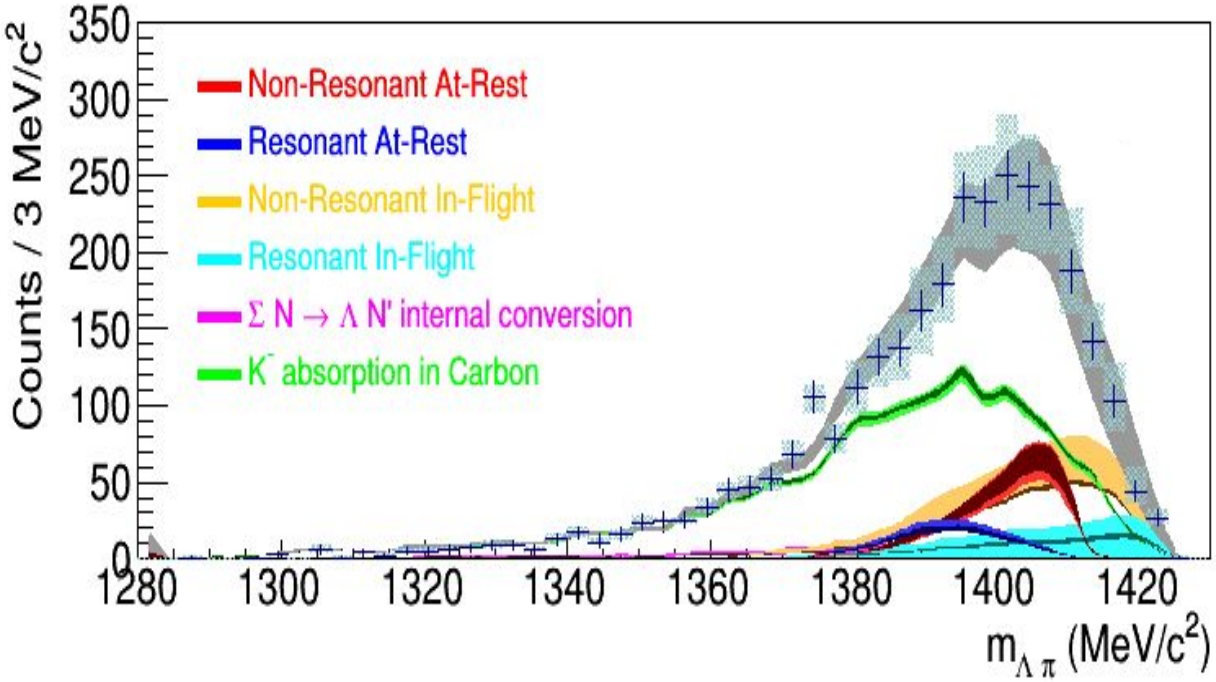

[K. Piscicchia, S. Wycech, L. Fabbietti et al. Phys.Lett. B782 (2018) 339-345]
[K. Piscicchia, S. Wycech, C. Curceanu, Nucl. Phys. A 954 (2016) 75-93]

Outcome of the measurement

Investigated using: **K⁻ "n"** ^{3}He → **Λπ⁻** ^{3}He

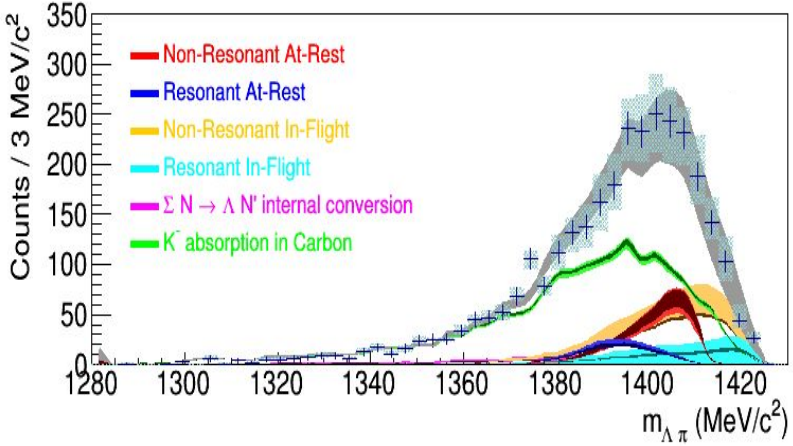

$$|f_{ar}^{nr}| = (0.334 \pm 0.018\,\mathrm{stat}^{+0.034}_{-0.058}\mathrm{syst})\ \mathrm{fm}$$

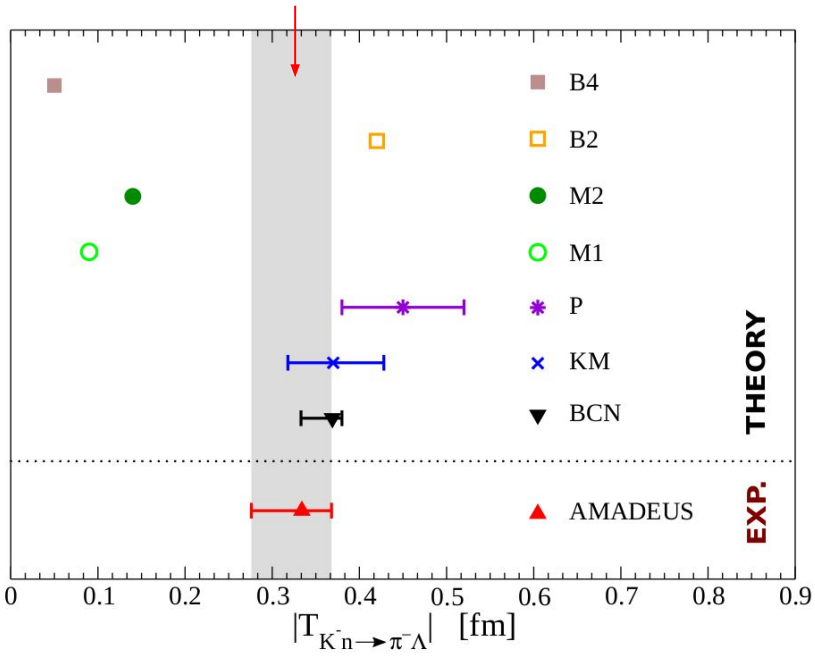

[K. Piscicchia, S. Wycech, L. Fabbietti et al. Phys.Lett. B782 (2018) 339-345]
[K. Piscicchia, S. Wycech, C. Curceanu, Nucl. Phys. A 954 (2016) 75-93]

Outcome of the measurement

Investigated using: **K⁻ "n"** ^{3}He → **Λπ⁻** ^{3}He

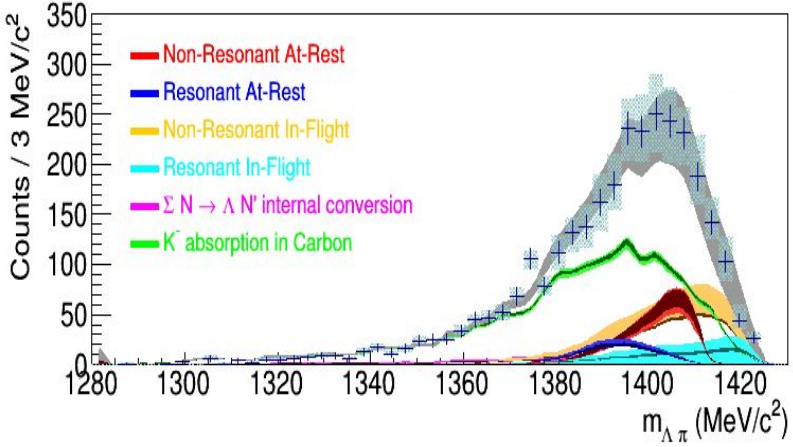

$$|f_{ar}^{nr}| = (0.334 \pm 0.018\,\mathrm{stat}^{+0.034}_{-0.058}\mathrm{syst})\ \mathrm{fm}$$

$E = -33$ MeV	$0.334 \pm 0.018\,\mathrm{stat}^{+0.034}_{-0.058}\mathrm{syst}$
$p_{lab} = 120$ MeV	0.33 ± 0.11
$p_{lab} = 160$ MeV	0.29 ± 0.10
$p_{lab} = 200$ MeV	0.24 ± 0.06
$p_{lab} = 245$ MeV	0.28 ± 0.02

TABLE II. The S-wave non-resonant amplitude ($|f^{nr}|$ fm) extracted from $K^-p \to \Lambda\pi^0$ scattering [34, 35] and from this experiment ($E = -33$ MeV).

J. K. Kim, Columbia University Report, Nevis 149 (1966)
J. K. Kim, Phys. Rev. Lett. 19 (1977) 1074

[K. Piscicchia, S. Wycech, L. Fabbietti et al. Phys.Lett. B782 (2018) 339-345]
[K. Piscicchia, S. Wycech, C. Curceanu, Nucl. Phys. A 954 (2016) 75-93]

Next step...

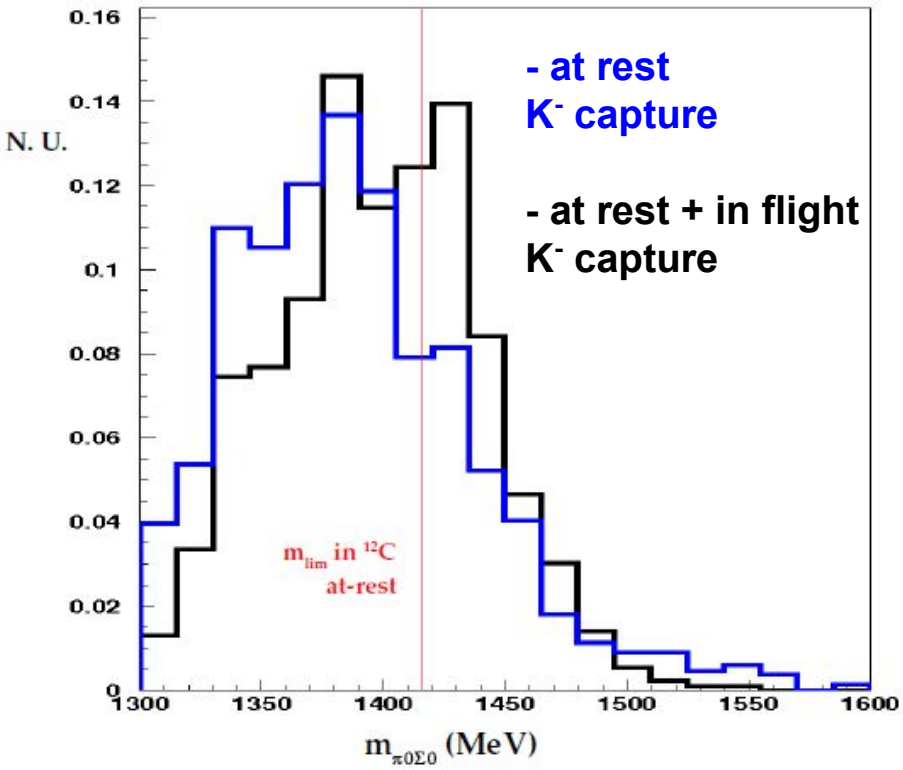

Same analysis for the I = 0 counterpart.

measured channel:

$$K^- p \rightarrow \Sigma^0 \pi^0$$

(bound proton in ^{12}C)

for the extraction of the $\Lambda(1405)$ shape

$p_{\pi 0}$ resolution: $\sigma_p \approx 12$ MeV/c

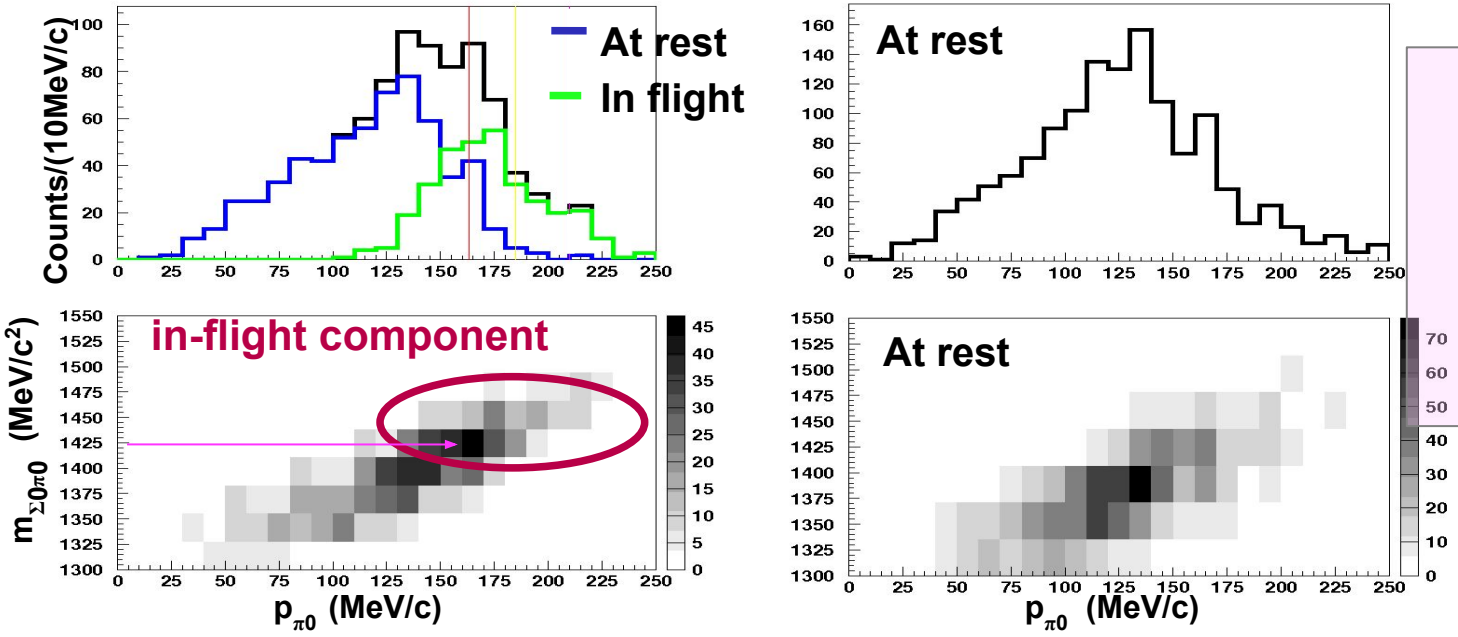

IN-FLIGHT

K- 12C

opens a window

between 1416 MeV

and K-Nth

difficulty: epoxy resin, contained in the carbon fibre target, contains H

H atoms in the molecules mainly contribute to **K- H absorption in-flight**, resulting in a **non-resonant background in the Σ^0 π^0 spectra**

measured channel: $K^- p \rightarrow \Sigma^+ \pi^-$ (bound proton in ^{12}C)

p_π resolution about 1MeV → K- capture at-rest/in-flight/on H can be distinguished

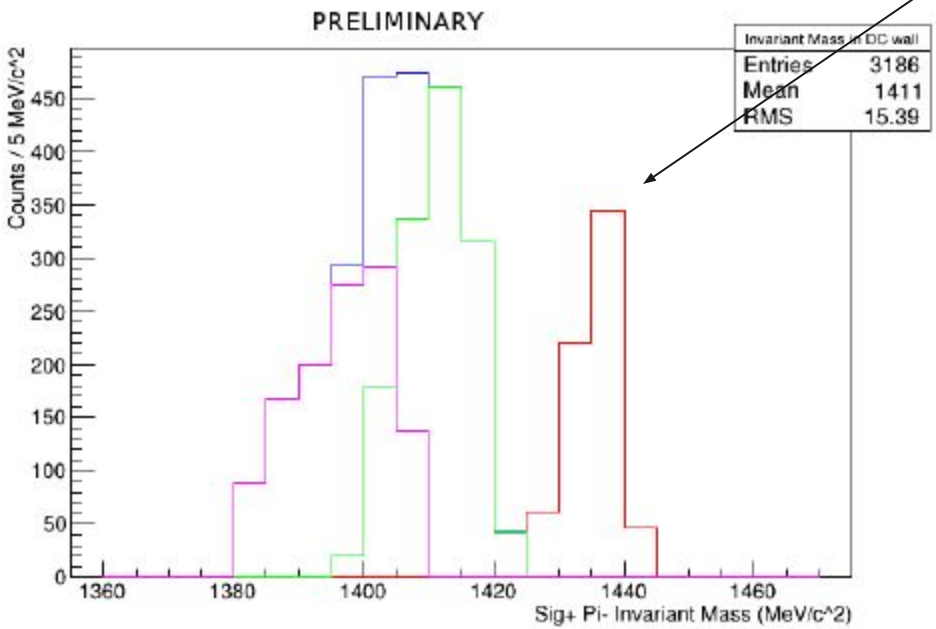

but, neglecting the small I = 2 component

$$\frac{d\sigma(\pi^+\Sigma^-)}{dM_I} \propto \frac{1}{3}|T^{(0)}|^2 + \frac{1}{2}|T^{(1)}|^2 + \frac{2}{\sqrt{6}}\mathrm{Re}\,(T^{(0)}T^{(1)*}),$$

$$\frac{d\sigma(\pi^-\Sigma^+)}{dM_I} \propto \frac{1}{3}|T^{(0)}|^2 + \frac{1}{2}|T^{(1)}|^2 - \frac{2}{\sqrt{6}}\mathrm{Re}\,(T^{(0)}T^{(1)*}),$$

$$\frac{d\sigma(\pi^0\Sigma^0)}{dM_I} \propto \frac{1}{3}|T^{(0)}|^2,$$

Figure 3: *(Colour online.) $m_{\Sigma\pi}$ invariant mass distributions in-flight (green) and at-rest (violet) in ^{12}C. Blue histogram represents the sum of green and violet histograms. The red distribution refers to K^- absorptions on Hydrogen*

Λ(1405) : extracting the resonant I = 0 contribution

PID optimised, data fit is ongoing

necessary the input of the $\Lambda\pi^-$ measurement

- K. Piscicchia et al., APP B48 (2017) 10, 1875
- C. Curceanu, K. Piscicchia et al., APP B46 (2015) 1, 203

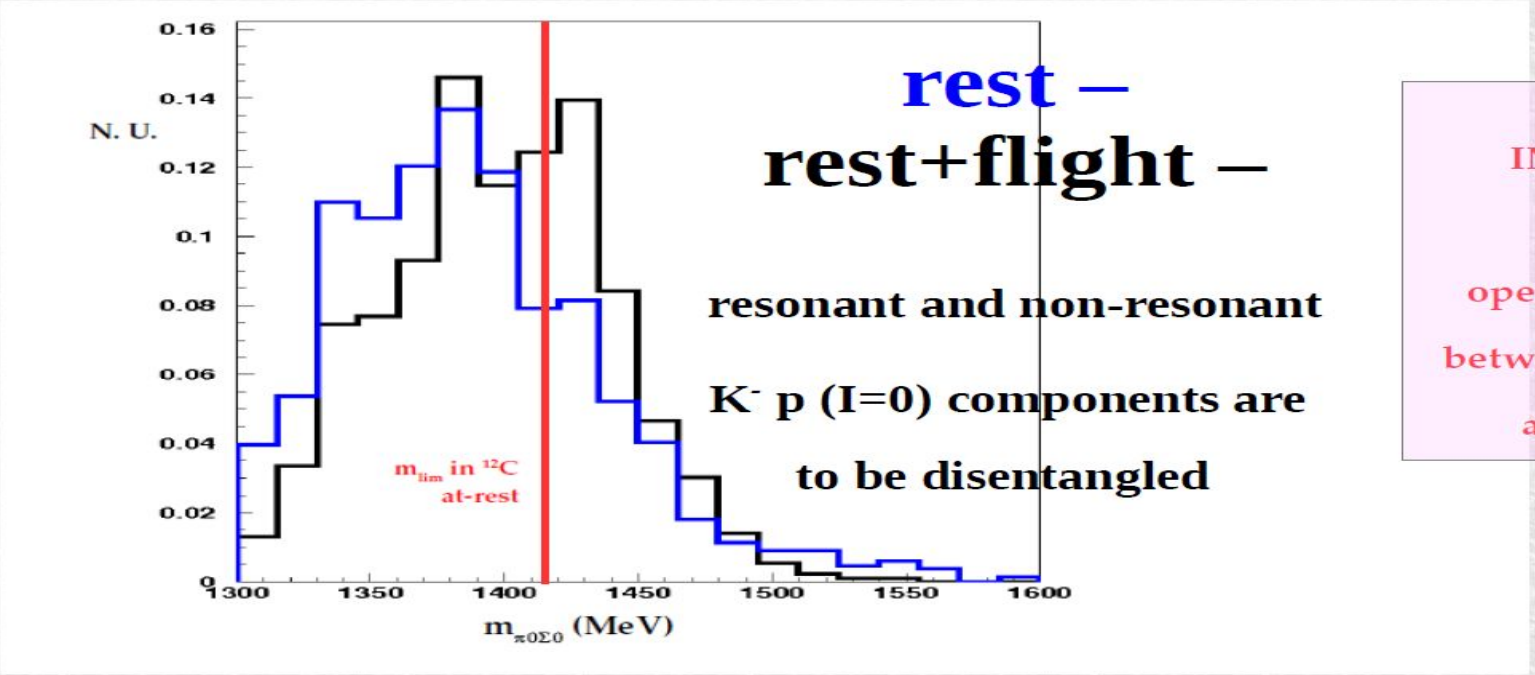

IN-FLIGHT

K- 12C

opens a window

between 1416 MeV

and K-Nth

Measurement of the Λ(1405) high mass pole in KN1 and KN2 experiments

Jido, D., Oset, E. & Sekihara, T. *Eur. Phys. J. A* 47, 42 (2011) see also Eur. Phys. J. A 42, 257 (2009):

$$K^- d \to \pi^0 \Sigma^0 n$$

- in flight reactions of low momentum (about 130 MeV) kaons, distinguish the resonant from non-resonant $\Sigma\pi$ production.

- Both the single scattering (non resonant) and the double scattering (resonant) give rise to a peak in the region of 1420 MeV.

- Single scattering is drastically reduced, in this region of inv. mass, at forward angles of the neutron, leading to a cleaner signal of the Λ(1405) resonance.

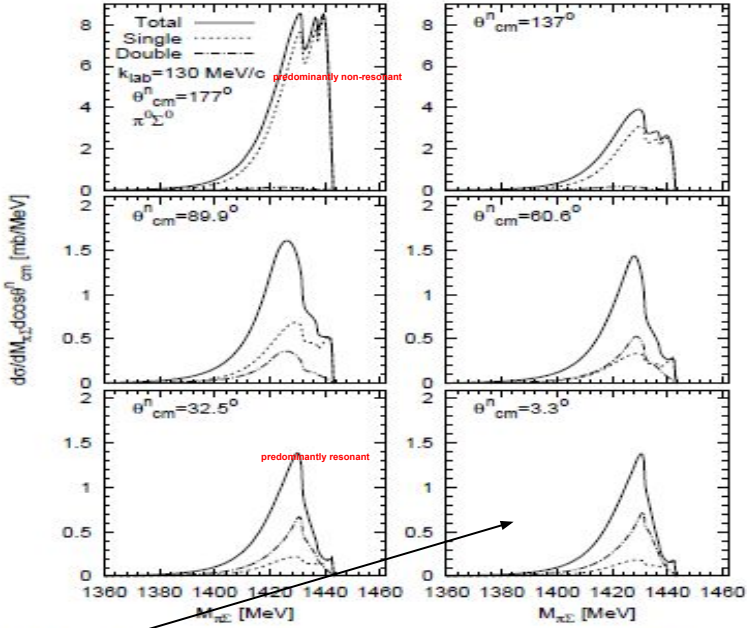

Fig. 5. Differential $\pi\Sigma$ invariant mass spectra of $K^- d \to \pi^0 \Sigma^0 n$ for 130 MeV/c of incident K^- momentum fixing the angle between the emitted neutron and the incident K^- in the CM frame. In each panel, the solid line denotes the total contributions of the three diagrams, while the dotted and dash-dotted lines show the calculations from the single and double scatterings, respectively.

- with the combination of the KN1 and KN2 detectors the kinematics of the K- d → $\Sigma^0\pi^0$ n reaction would be closed,

- forward neutrons (angle between the outgoing neutron and the incident K- in the CM frame) can be selected

- optimization of the neutrals detector ongoing based on MC simulations.

- simulation of the neutrons momentum distribution for the non-resonant process, (simulation for double scattering ongoing):

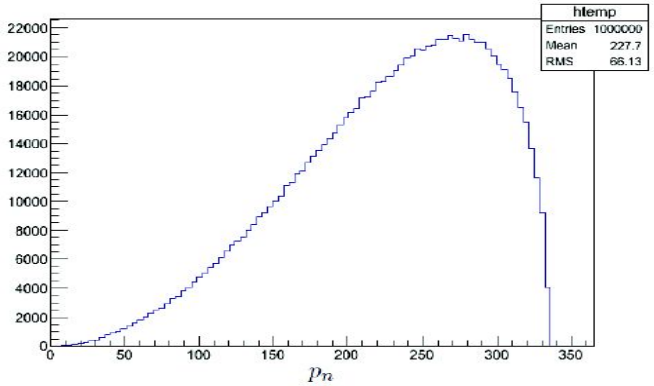

Fig. 6. *neutrons momentum distribution.*

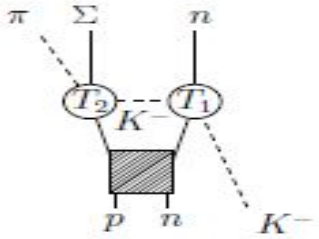

in double scattering the neutron gets some energy from the K^- → higher efficiency.

Summary

K^-n amplitude below threshold

$$|f^s_{ar}| = (0.334 \pm 0.018\,\mathrm{stat}^{+0.034}_{-0.058}\mathrm{syst})\ \mathrm{fm}\,.$$

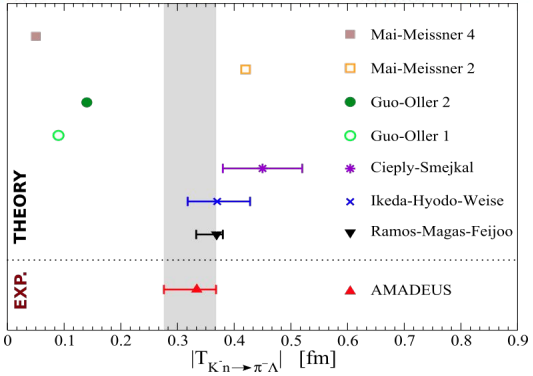

Λ p channel: 2NA, 3NA and 4NA BRs and σ

Process	Branching Ratio (%)	σ (mb)	@	p_K (MeV/c)
2NA-QF Λp	0.25 ± 0.02 (stat.) $^{+0.01}_{-0.02}$(syst.)	2.8 ± 0.3 (stat.) $^{+0.1}_{-0.2}$ (syst.)	@	128 ± 29
2NA-FSI Λp	6.2 ± 1.4(stat.) $^{+0.5}_{-0.6}$(syst.)	69 ± 15 (stat.) ± 6 (syst.)	@	128 ± 29
2NA-QF Σ^0p	0.35 ± 0.09(stat.) $^{+0.13}_{-0.06}$(syst.)	3.9 ± 1.0 (stat.) $^{+1.4}_{-0.7}$ (syst.)	@	128 ± 29
2NA-FSI Σ^0p	7.2 ± 2.2(stat.) $^{+4.2}_{-5.4}$(syst.)	80 ± 25 (stat.) $^{+46}_{-60}$ (syst.)	@	128 ± 29
2NA-CONV Σ/Λ	2.1 ± 1.2(stat.) $^{+0.9}_{-0.5}$(syst.)	-		
3NA Λpn	1.4 ± 0.2(stat.) $^{+0.1}_{-0.2}$(syst.)	15 ± 2 (stat.) ± 2 (syst.)	@	117 ± 23
3NA Σ^0pn	3.7 ± 0.4(stat.) $^{+0.2}_{-0.4}$(syst.)	41 ± 4 (stat.) $^{+2}_{-5}$ (syst.)	@	117 ± 23
4NA Λpnn	0.13 ± 0.09(stat.) $^{+0.08}_{-0.07}$(syst.)	-		
Global Λ(Σ^0)p	21 ± 3(stat.) $^{+5}_{-6}$(syst.)	-		

Λ t channel: 4NA BRs and σ

BR(K^{-4}He(4NA) → Λt) < 2.0×10^{-4} /K_{stop} (95% c. l.)

σ(100 ± 19 MeV/c) (K^{-4}He(4NA) →Λt) =

= (0.81 ± 0.21 (stat) $^{+0.03}_{-0.04}$ (syst)) mb

BR(K^{-12}C(4NA) → Λt ^{8}Be) = $1.5 \pm 0.5 \times 10^{-4}$ (stat) /K_{stop}

σ(K^{-12}C (4NA) →Λt ^{8}Be) = 0.58 ± 0.11 (stat) mb

σ(K^{-12}C (4NA) →Σ^0t ^{8}Be) = 1.88 ± 0.35 (stat) mb

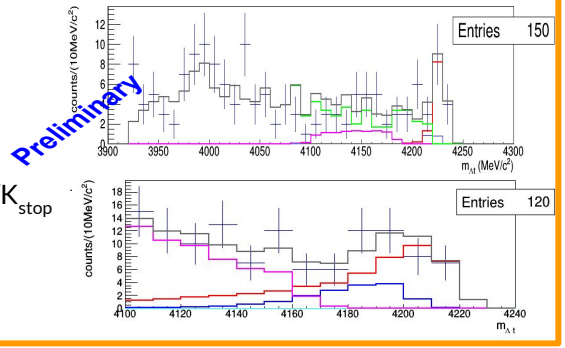

Thank You